

Threshold corrections to the MSSM finite-temperature Higgs potential

M. Dolgoplov[‡], M. Dubinin^{*}, E. Rykova[‡]

[‡] *Samara State University, 443011 Samara, Russia*

^{*} *Skobeltsyn Institute of Nuclear Physics, Moscow State University, 119991 Moscow, Russia*

Abstract

In the minimal supersymmetric standard model (MSSM) the one-loop finite-temperature corrections from the squarks-Higgs bosons sector are calculated, the effective two-Higgs-doublet potential is reconstructed and possibilities of the electroweak phase transition in full MSSM (m_{H^\pm} , $\tan\beta$, $A_{t,b}$, μ , m_Q , m_U , m_D) parameter space are studied. At large values of $A_{t,b}$ and μ of around 1 TeV, favored indirectly by LEP2 and Tevatron data, the threshold finite-temperature corrections from triangle and box diagrams with intermediate third generation squarks are very substantial. Four types of bifurcation sets are defined for the two-Higgs-doublet potential. High sensitivity of the low-temperature evolution to the effective two-doublet and the MSSM squark sector parameters is observed, but rather extensive regions of the full MSSM parameter space allow the first-order electroweak phase transition respecting the phenomenological constraints at zero temperature. As a rule, these regions of the MSSM parameter space are in line with the case of a light stop quark.

PACS:

Keywords: supersymmetry, Higgs boson, electroweak phase transition, critical temperature

1 Introduction

The absence of antimatter in the Universe (the baryon asymmetry), a small ratio of the observed number of baryons to the observed number of photons $n_B/n_\gamma \sim 6 \times 10^{-10}$ and the absence of light ($m_H \sim 100$ GeV) CP-even Higgs boson signal at LEP2 and Tevatron energies lay a specific claim to models of particle physics. The baryon asymmetry and an extremely small n_B/n_γ could be understood on the basis of Sakharov conditions, which are respected at the electroweak phase transition, expected to take place at the temperature of the order of 10^2 GeV [1]. Generation of nonzero vacuum expectation value v of the scalar field breaks the electroweak symmetry $SU(2)_f \times U(1)_Y$ to the electromagnetic symmetry $U(1)_{em}$. It is well-known [2] that in the simple isoscalar model with the standard-like Higgs potential $U(\varphi) = -\frac{1}{2}\mu^2\varphi^2 + \frac{1}{4}\lambda\varphi^4$, describing a thermodynamically equilibrium system of the scalar particles at the temperature T , the equation for the vacuum expectation value $v(T)$ has two solutions: $v(0) = 0$ and $v^2(T) = \mu^2/\lambda - T^2/4$, demonstrating the second order phase transition at the critical temperature $T_c = 2\mu/\sqrt{\lambda} = 2v(0)$, see Fig.1a. The thermal Higgs boson mass $m_h^2 = -\mu^2 + \lambda T^2/4$ vanishes at the critical temperature T_c thus restoring the spontaneously broken symmetry.

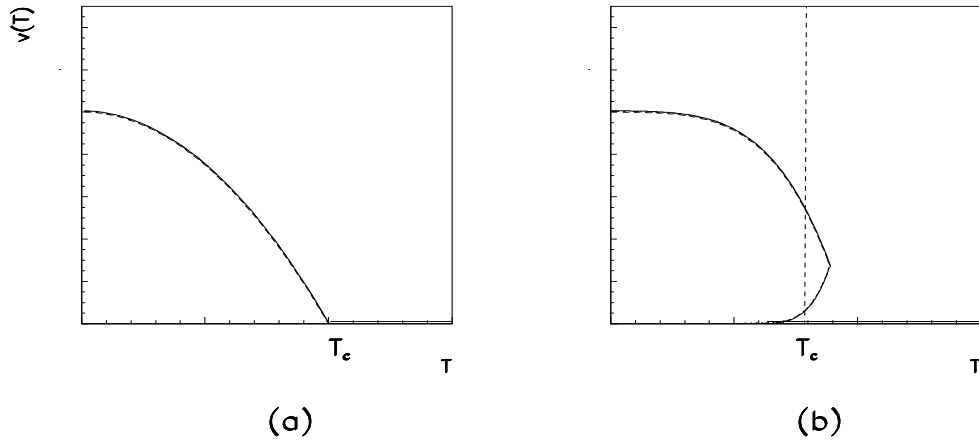


Figure 1: Contours on the (v, T) plane for (a) the second order phase transition (fracture point) and (b) the first order phase transition at the critical temperature T_c (dashed vertical line).

However, in the cosmological evolution the stages with thermodynamically non equilibrium plasma and the first order phase transitions (see a typical $v(T)$ contour in Fig.1b) are very important, so such simple picture in combination with the standard model CP-violation by means of the CKM mixing matrix turns out to be not sufficient to justify the observed ratio of baryon number to entropy. The situation becomes better in the minimal supersymmetric model (MSSM) where sparticles, extended two-doublet Higgs sector with the two background fields and nonstandard sources of CP-violation provide a number of new possibilities. In a number of approaches [3] the electroweak phase transition is defined by evolution of the finite temperature effective Higgs potential involving the cubic term in the background scalar fields v_1, v_2 . The larger this term is, the stronger pronounced turns out to be the first order phase transition, which is essential for consistency with the Higgs boson mass beyond the LEP2 exclusion $m_H < 115$ GeV. Enhancement of the cubic term in the MSSM at the one-loop level is substantial in the class of MSSM scenarios with a light right stop [4]. Temperature loop corrections from the stop and other additional scalar states could be large and lead to the first order phase transition, the intensity of the latter depends on $\xi = v(T_c)/T_c$, where $v(T_c) = \sqrt{v_1^2(T_c) + v_2^2(T_c)}$ is the

vacuum expectation value at the critical temperature T_c . The electroweak baryogenesis could be explained if $v(T_c)/T_c > 1$ [5], the case of strong first order phase transition.

In a number of analyses the MSSM finite-temperature effective potential is taken in the representation

$$V_{eff}(v, T) = V_0(v_1, v_2, 0) + V_1(m(v), 0) + V_1(T) + V_{ring}(T), \quad (1)$$

where V_0 is the tree-level MSSM two-doublet potential at the SUSY scale, V_1 is the (non-temperature) one-loop resummed Coleman-Weinberg term, dominated by stop and sbottom contributions, $V_1(T)$ is the one-loop temperature term and V_{ring} is the correction of re-summed leading infrared contribution from multi-loop ring (or daisy) diagrams. The MSSM relations between the $SU(2)_L \times U(1)_Y$ gauge couplings g_2 and g_1 , and the quartic parameters $\lambda_{1,2,3,4}$ of the potential $V_0(v_1, v_2, 0)$ are very restrictive. Only two additional parameters $\tan\beta = v_2/v_1$ and m_{H^\pm} (charged scalar mass) determine the zero-temperature two-doublet Higgs sector at tree-level. The one-loop radiative corrections, both logarithmic and non-logarithmic generated at the threshold M_{SUSY} , can change strongly the tree-level picture. They depend on the parameters ($A_{t,b}$, μ , m_Q , m_U , m_D) of the scalar quarks-Higgs bosons interaction sector. In most cases for the analysis in the representation (1) numerical methods are used to find the critical temperature T_c , for example, by solving the equation for the determinant of second derivatives of the potential (1) at $v_{1,2} = 0$ [6]. Then the two background fields $v_{1,2}(T_c)$ are found at the minimum using the minimization conditions (i.e. the absence of linear terms of the effective potential representation in the "shifted" fields). The first order phase transition strength is dependent on the cubic term ETv^3 which appears from the infrared region.

Numerical high-precision Monte Carlo simulations on the lattice [7] have been developed and applied to MSSM in connection with the infrared problem [8] inherent to all analyses based on the effective potentials. Infrared divergences appear in the integration over bosonic static ($\omega_0 = 0$) Matsubara modes, which in the loop expansion for the three-dimensional momentum space correspond to the intermediate massless bosons. The non-perturbative investigations of the problem have been performed in the framework of high-temperature dimensional reduction [9, 10], when an effective three-dimensional MSSM with the same Green's functions as in the four-dimensional MSSM for the light bosons is constructed [11, 12, 13] by integrating out perturbatively the non-static modes. The corrections from squarks and gauge bosons are introduced after the reduction to the three-dimensional model.

In order to cover the temperature range from very low temperatures to the temperatures of the order of critical, the following analysis uses an approach developed in [14, 15] for the general (non-temperature) two-Higgs doublet potential with complex-valued parameters μ_{12}^2 , λ_5 , λ_6 and λ_7 , which violates the CP-invariance explicitly. However, in this publication a simplified situation of the Higgs potential in the CP conserving limit is considered (the imaginary parts of the effective parameters $\lambda_{5,6,7}$ and μ_{12}^2 are taken to be zero). Full MSSM effective potential in the generic Φ_1 , Φ_2 basis has the form

$$\begin{aligned} U_{eff}(\Phi_1, \Phi_2) = & -\mu_1^2(\Phi_1^\dagger\Phi_1) - \mu_2^2(\Phi_2^\dagger\Phi_2) - \mu_{12}^2(\Phi_1^\dagger\Phi_2) - \mu_{12}^{*2}(\Phi_2^\dagger\Phi_1) + \lambda_1(\Phi_1^\dagger\Phi_1)^2 + \lambda_2(\Phi_2^\dagger\Phi_2)^2 \quad (2) \\ & + \lambda_3(\Phi_1^\dagger\Phi_1)(\Phi_2^\dagger\Phi_2) + \lambda_4(\Phi_1^\dagger\Phi_2)(\Phi_2^\dagger\Phi_1) + \frac{\lambda_5}{2}(\Phi_1^\dagger\Phi_2)(\Phi_1^\dagger\Phi_2) + \frac{\lambda_5^*}{2}(\Phi_2^\dagger\Phi_1)(\Phi_2^\dagger\Phi_1) + \\ & + \lambda_6(\Phi_1^\dagger\Phi_1)(\Phi_1^\dagger\Phi_2) + \lambda_6^*(\Phi_1^\dagger\Phi_1)(\Phi_2^\dagger\Phi_1) + \lambda_7(\Phi_2^\dagger\Phi_2)(\Phi_1^\dagger\Phi_2) + \lambda_7^*(\Phi_2^\dagger\Phi_2)(\Phi_2^\dagger\Phi_1) \end{aligned}$$

where the background fields (vev's) are $\langle\Phi_1\rangle = (0, v_1)/\sqrt{2}$ and $\langle\Phi_2\rangle = (0, v_2)/\sqrt{2}$. The temperature corrections from squarks, both logarithmic and non-logarithmic (at the SUSY threshold)

are incorporated to $\lambda_1, \dots, \lambda_7$. In [14, 15] (see also [16]) a nonlinear transformation for masses and mixing angles $\lambda_i = \lambda_i(\alpha, \beta, m_h, m_H, m_A, m_{H^\pm}, \lambda_6, \lambda_7)$, $i = 1, \dots, 5$ to the Higgs bosons mass basis can be found for a general case (h, H and A are the neutral and H^+ , H^- are the charged Higgs bosons, α is the h - H mixing angle, $\tan\beta = v_2/v_1$)

$$U_{eff}(\Phi_1, \Phi_2) \implies \frac{m_h^2}{2}(hh) + \frac{m_H^2}{2}(HH) + \frac{m_A^2}{2}(AA) + m_{H^\pm}^2(H^+H^-) + h, H, A, H^\pm \quad \text{interaction terms} \quad (3)$$

which allows to work with symbolic expressions for the temperature-dependent Higgs boson mass eigenstates.

In section 2 various one-loop temperature corrections to the potential are calculated. Section 3 contains some examples of the electroweak phase transition for the finite-temperature effective potential reconstructed in the full MSSM parameter space. The potential of scalar quarks - Higgs bosons interaction and some technical details of evaluation can be found in the Appendix.

2 Finite temperature corrections of squarks

In the finite temperature field theory Feynman diagrams with boson propagators, containing Matsubara frequencies $\omega_n = 2\pi nT$ ($n = 0, \pm 1, \pm 2, \dots$), lead to structures of the form

$$I[m_1, m_2, \dots, m_b] = T \sum_{n=-\infty}^{\infty} \int \frac{d\mathbf{k}}{(2\pi)^3} \prod_{i=1}^b \frac{(-1)^b}{(\mathbf{k}^2 + \omega_n^2 + m_i^2)}, \quad (4)$$

Here \mathbf{k} is the three-dimensional momentum in a system with the temperature T . In the following calculations first we perform integration with respect to \mathbf{k} and then take the sum, using the reduction to three-dimensional theory in the high-temperature limit for zero frequencies. At $n \neq 0$ the result is [17, 18]

$$I[m_1, m_2, \dots, m_b] = 2T (2\pi T)^{3-2b} \frac{(-1)^b \pi^{3/2}}{(2\pi)^3} \frac{\Gamma(b-3/2)}{\Gamma(b)} S(M, b-3/2), \quad (5)$$

where

$$S(M, b-3/2) = \int \{dx\} \sum_{n=1}^{\infty} \frac{1}{(n^2 + M^2)^{b-3/2}}, \quad M^2 \equiv \left(\frac{m}{2\pi T}\right)^2. \quad (6)$$

For $b > 1$ the parameter m^2 is a linear function dependent on m_i^2 and the variables $\{dx\}$ of Feynman parametrization, which are the integration variables in (6). At the integer values of b the integrand in (3) is a generalized Hurwitz zeta-function [19]. Note that for the leading threshold corrections to effective parameters of the two-doublet potential $b > 2$, so the wave-function renormalization appears in connection with the divergence at $b = 2$ (which is suppressed by vertex factors, see [14]).

A number of integrals can be easily calculated. The integral J_0 is calculated

$$J_0[a_1, a_2] = \int \frac{d\mathbf{k}}{(2\pi)^3} \frac{1}{(\mathbf{k}^2 + a_1^2)(\mathbf{k}^2 + a_2^2)} = \frac{1}{4\pi(a_1 + a_2)}, \quad (7)$$

taking a residue in the spherical coordinate system. Here $a_{1,2}^2$ are the sums of squared frequency and squared mass, see (4). Derivatives of J_0 with respect to a_1 and a_2 can be used for calculation of integrals

$$J_1[a_1, a_2] = \int \frac{d\mathbf{k}}{(2\pi)^3} \frac{1}{(\mathbf{k}^2 + a_1^2)^2(\mathbf{k}^2 + a_2^2)} = -\frac{1}{2a_1} \frac{\partial J_0}{\partial a_1} = \frac{1}{8\pi a_1(a_1 + a_2)^2}, \quad (8)$$

$$J_2[a_1, a_2] = \int \frac{d\mathbf{k}}{(2\pi)^3} \frac{1}{(\mathbf{k}^2 + a_1^2)^2(\mathbf{k}^2 + a_2^2)^2} = \frac{1}{4a_1a_2} \frac{\partial^2 J_0}{\partial a_1 \partial a_2} = \frac{1}{8\pi a_1 a_2 (a_1 + a_2)^3}, \quad (9)$$

and ¹

$$J_3[a_1, a_2, a_3] = \int \frac{d\mathbf{k}}{(2\pi)^3} \frac{1}{(\mathbf{k}^2 + a_1^2)(\mathbf{k}^2 + a_2^2)(\mathbf{k}^2 + a_3^2)} = \frac{1}{4\pi(a_1 + a_2)(a_1 + a_3)(a_2 + a_3)}, \quad (10)$$

$$J_4[a_1, a_2, a_3] = \int \frac{d\mathbf{k}}{(2\pi)^3} \frac{1}{(\mathbf{k}^2 + a_1^2)^2(\mathbf{k}^2 + a_2^2)(\mathbf{k}^2 + a_3^2)} = \frac{2a_1 + a_2 + a_3}{8\pi a_1(a_1 + a_2)^2(a_1 + a_3)^2(a_2 + a_3)}, \quad (11)$$

Thus, the procedure of Feynman parametrization is not used. Substitution of $a_1^2 = 4\pi^2 n^2 T^2 + m_1^2$ and $a_2^2 = 4\pi^2 n^2 T^2 + m_2^2$ to (7) and summation over Matsubara frequencies after the integration gives

$$I_0[m_1, m_2] = \sum_{n=-\infty, n \neq 0}^{\infty} J_0^n[m_1, m_2] = \sum_{n=-\infty, n \neq 0}^{\infty} \frac{1}{4\pi(\sqrt{4\pi^2 n^2 T^2 + m_1^2} + \sqrt{4\pi^2 n^2 T^2 + m_2^2})}. \quad (12)$$

or, after redefinition of mass parameters $M_{1;2} = m_{1;2}/2\pi T$ the temperature corrections to effective potential are expressed by summed integrals

$$I_1[M_1, M_2] = -\frac{1}{64\pi^4 T^2} \sum_{n=-\infty, n \neq 0}^{\infty} \frac{1}{\sqrt{M_1^2 + n^2}(\sqrt{M_1^2 + n^2} + \sqrt{M_2^2 + n^2})^2}, \quad (13)$$

$$I_2[M_1, M_2] = \frac{1}{256\pi^5 T^4} \sum_{n=-\infty, n \neq 0}^{\infty} \frac{1}{\sqrt{M_1^2 + n^2} \sqrt{M_2^2 + n^2} (\sqrt{M_1^2 + n^2} + \sqrt{M_2^2 + n^2})^3}. \quad (14)$$

Note that the series (12) are divergent, but the derivatives (13) and (14) are convergent for all $M_{1;2}$. In the following it will be convenient to keep separately terms for zero and nonzero modes in the sum. Both terms will be temperature-dependent since the zero-mode integrals coincide with (7)-(9), where $a_i^2 = m_i^2$ and the factor T should be accounted for. Numerical check of the zero temperature limiting case $T \rightarrow 0$ demonstrates that the non-temperature field theory results are successfully reproduced. In the high-temperature limit the zero mode gives dominant contribution in agreement with a known suppression of quantum effects at increasing temperatures.

The sum of integrals (13) and (14) can be expressed by means of the generalized zeta-function. Such forms can be derived if we introduce Feynman parameters in the integrand of (7)

$$\frac{1}{[\mathbf{k}^2 + m_a^2][\mathbf{k}^2 + m_b^2]} = \int_0^1 \frac{dx}{([\mathbf{k}^2 + m_a^2]x + [\mathbf{k}^2 + m_b^2](1-x))^2}, \quad (15)$$

and redefine $\mathbf{k} \rightarrow \mathbf{p} = \mathbf{k}/2\pi T$, $M^2(M_a, M_b, x) = (M_a^2 - M_b^2)x + M_b^2$. Then we get

$$\frac{1}{[\mathbf{k}^2 + m_a^2][\mathbf{k}^2 + m_b^2]} = \frac{1}{(2\pi T)^4} \int_0^1 \frac{dx}{(\mathbf{p}^2 + n^2 + M^2)^2}. \quad (16)$$

and divergent series for (7) ($d\mathbf{k} = (2\pi T)^3 d\mathbf{p}$)

$$I_0[M_a, M_b] = \frac{1}{2\pi T} \int_0^1 dx \sum_{n=-\infty, n \neq 0}^{\infty} \int \frac{d\mathbf{p}}{(2\pi)^3} \frac{1}{(\mathbf{p}^2 + n^2 + M^2)^2}, \quad (17)$$

¹The same results for J_3 and J_4 can be found in [11] and [12], where they appear in the context of high temperature dimensional reduction.

With the help of dimensional regularization or differentiating the integral

$$\int \frac{d\mathbf{p}}{(2\pi)^3} \frac{1}{(\mathbf{p}^2 + M^2)} = -\frac{M}{4\pi} + \mathcal{O}\left(\frac{M^2}{T^2}\right) \quad (18)$$

over the parameter M , the equation (17) can be reduced to

$$I_0[M_a, M_b] = \frac{1}{16\pi^2 T} \int_0^1 dx \zeta\left(2, \frac{1}{2}, M^2\right), \quad (19)$$

where $\zeta(u, s, t)$ is the generalized Hurwitz zeta-function [19]: ²

$$\zeta(u, s, t) = \sum_{n=1}^{\infty} \frac{1}{(n^u + t)^s}. \quad (20)$$

So in the case under consideration the sums of integrals (13) and (14) can be calculated by differentiation of (19) with respect to mass parameters participating in $M = M(M_a, M_b, x)$. Differentiation increases the power s in the denominator of (19) giving convergent integrals

$$I_1[M_a, M_b] = \frac{T}{2M_a} \frac{\partial}{\partial M_a} I_0 = -\frac{1}{64\pi^4 T^2} \int_0^1 dx x \zeta\left[2, \frac{3}{2}, M^2(x)\right], \quad (21)$$

$$I_2[M_a, M_b] = -\frac{1}{2M_b} \frac{\partial}{\partial M_b} (-I_1) = \frac{3}{256\pi^6 T^4} \int_0^1 dx x (1-x) \zeta\left[2, \frac{5}{2}, M^2(x)\right]. \quad (22)$$

The integrals (21) and (22) are equal to the series (13) and (14), respectively.

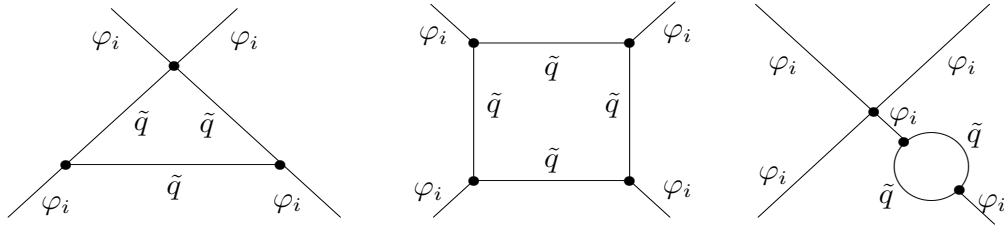


Figure 2: Threshold corrections (left and central diagram) and diagram contributing to the wave-function renormalization (right).

Threshold corrections from the triangle and box diagrams, shown in Fig.2, are denoted by $\Delta\lambda_i^{th}$, $i=1, \dots, 7$. They contribute additively to the parameters $\lambda_i = \lambda_i^{SUSY} - \Delta\lambda_i^{th}$. In the following normalization conventions from [14] are used. Calculation of the finite-temperature diagrams for the general case of complex-valued μ and $A_{t,b}$ gives the result (see details in the Appendix)

$$\begin{aligned} \Delta\lambda_1^{thr} = & 3h_t^4 |\mu|^4 I_2[m_Q, m_U] + 3h_b^4 |A_b|^4 I_2[m_Q, m_D] + \\ & + h_t^2 |\mu|^2 \left(-\frac{g_1^2 - 3g_2^2}{2} I_1[m_Q, m_U] + 2g_1^2 I_1[m_U, m_Q] \right) \end{aligned} \quad (23)$$

²Note that (non-generalized) Hurwitz zeta-function is defined by $\zeta(s, t) = \sum_{n=0}^{\infty} \frac{1}{[n+t]^s}$.

$$\begin{aligned}
& +h_b^2|A_b|^2\left(\frac{12h_b^2-g_1^2-3g_2^2}{2}I_1[m_Q, m_D] + (6h_b^2-g_1^2)I_1[m_D, m_Q]\right) \\
& \Delta\lambda_2^{thr} = 3h_t^4|A_t|^4I_2[m_Q, m_U] + 3h_b^4|\mu|^4I_2[m_Q, m_D] + \\
& +h_b^2|\mu|^2\left(\frac{g_1^2+3g_2^2}{2}I_1[m_Q, m_D] + g_1^2I_1[m_D, m_Q]\right) + \\
& +h_t^2|A_t|^2\left(\frac{12h_t^2+g_1^2-3g_2^2}{2}I_1[m_Q, m_U] + (6h_t^2-2g_1^2)I_1[m_U, m_Q]\right)
\end{aligned} \tag{24}$$

$$\begin{aligned}
\Delta\lambda_3^{thr} = & h_t^2\left(|\mu|^2\frac{3g_2^2+g_1^2}{12} + |A_t|^2\frac{12h_t^2-g_1^2-3g_2^2}{12}\right)I_1[m_Q, m_U] + \\
& +\left(|\mu|^2\frac{3h_t^2-g_1^2}{3} + |A_t|^2\frac{g_1^2}{3}\right)I_1[m_U, m_Q] + \\
& +\left(h_b^2\left(|\mu|^2\frac{3g_2^2-g_1^2}{12} + |A_b|^2\frac{12h_b^2+g_1^2-3g_2^2}{4}\right)I_1[m_Q, m_D] + \right. \\
& \left. +\left(|\mu|^2\frac{6h_b^2-g_1^2}{6} + |A_b|^2\frac{g_1^2}{6}\right)I_1[m_D, m_Q]\right) + \\
& +h_t^2|\mu|^2|A_t|^2I_2[m_Q, m_U] + h_b^2|\mu|^2|A_b|^2I_2[m_Q, m_D] + \\
& +h_t^2h_b^2(2(A_tA_b-|\mu|^2)I_3[m_Q, m_U, m_D] + (|\mu|^4+|A_t|^2|A_b|^2-2A_tA_b|\mu|^2)I_4[m_Q, m_U, m_D])
\end{aligned} \tag{25}$$

$$\begin{aligned}
\Delta\lambda_4^{thr} = & 6h_t^4|\mu|^2|A_t|^2I_2[m_Q, m_U] + 6h_b^4|\mu|^2|A_b|^2I_2[m_Q, m_D] + \\
& +h_t^2\left(|\mu|^2\frac{12h_t^2+g_1^2-3g_2^2}{4} - |A_t|^2\frac{g_1^2-3g_2^2}{4}\right)I_1[m_Q, m_U] + \\
& +(|A_t|^2g_1^2-|\mu|^2(g_1^2-3h_t^2))I_1[m_U, m_Q] + \\
& +h_b^2\left(|\mu|^2\frac{-12h_b^2+g_1^2+3g_2^2}{4} - |A_b|^2\frac{g_1^2+3g_2^2}{4}\right)I_1[m_Q, m_D] + \\
& +\frac{1}{2}(|A_b|^2g_1^2-|\mu|^2(g_1^2-6h_b^2))I_1[m_D, m_Q] - \Delta\lambda_3^{th}
\end{aligned} \tag{26}$$

$$\Delta\lambda_5^{thr} = 3h_t^4\mu^2A_t^2I_2[m_Q, m_U] + 3h_b^4\mu^2A_b^2I_2[m_Q, m_D] \tag{27}$$

$$\Delta\lambda_6^{thr} = -3h_t^4\mu A_t|\mu|^2I_2[m_Q, m_U] - 3h_b^4\mu A_b|A_b|^2I_2[m_Q, m_D] + \tag{28}$$

$$\begin{aligned}
& +h_t^2\mu A_t\left(\frac{g_1^2-3g_2^2}{4}I_1[m_Q, m_U] - g_1^2I_1[m_U, m_Q]\right) + \\
& +h_b^2\mu A_b\left(\frac{-12h_b^2+g_1^2+3g_2^2}{4}I_1[m_Q, m_D] - \frac{6h_b^2-g_1^2}{2}I_1[m_D, m_Q]\right) \\
& \Delta\lambda_7^{thr} = -3h_t^4\mu A_t|A_t|^2I_2[m_Q, m_U] - 3h_b^4\mu A_b|\mu|^2I_2[m_Q, m_D] \\
& +h_b^2\mu A_b\left(-\frac{g_1^2+3g_2^2}{4}I_1[m_Q, m_D] - \frac{g_1^2}{2}I_1[m_D, m_Q]\right) + \\
& +h_t^2\mu A_t\left(\frac{12h_t^2+g_1^2-3g_2^2}{4}I_1[m_Q, m_U] - (3h_t^2-g_1^2)I_1[m_U, m_Q]\right)
\end{aligned} \tag{29}$$

where g_1, g_2 are U(1) and SU(2) gauge couplings, μ is the Higgs superfield mass parameter, A_t, A_b are the trilinear squarks-Higgs bosons parameters, h_t, h_b are the Yukawa couplings and

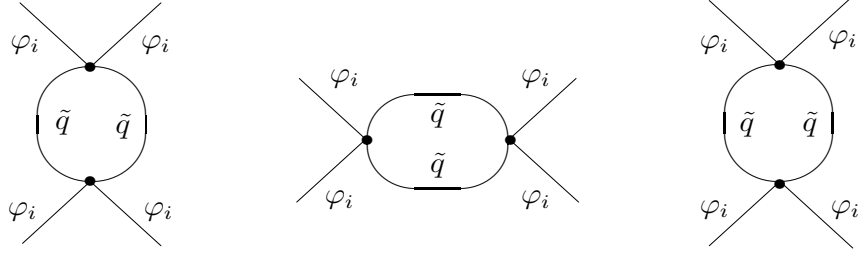


Figure 3: "Fish" diagrams

m_Q, m_U, m_D denote the scalar quark mass parameters, in terms of which the physical masses are expressed.

Corrections of "fish" diagrams, see Fig.3, give the following contributions to the effective parameters

$$-\Delta\lambda_1^f = \left[h_b^2 - \frac{g_1^2}{6} \right]^2 (I(m_Q) + I(m_D)) + \frac{g_1^4}{9} I(m_U), \quad (30)$$

$$-\Delta\lambda_2^f = \left[h_t^2 + \frac{g_1^2}{6} \right]^2 I(m_Q) + [h_t^2 - \frac{g_1^2}{3}]^2 I(m_U) + \frac{g_1^4}{36} I(m_D), \quad (31)$$

$$\begin{aligned} -(\Delta\lambda_3 + \Delta\lambda_4)^f &= \frac{1}{72} \left(-g_1^4 + 6(h_b^2 - h_t^2)g_1^2 - 9(g_2^4 - 2(h_b^2 + h_t^2)g_2^2) \right) I(m_Q) + \\ &+ \frac{g_1^2}{3} (h_t^2 - \frac{g_1^2}{3}) I(m_U) + \frac{g_1^2}{6} (h_b^2 - \frac{g_1^2}{6}) I(m_D), \end{aligned} \quad (32)$$

$$\begin{aligned} -\Delta\lambda_3^f &= \frac{1}{72} \left(-g_1^4 + 6(h_b^2 - h_t^2)g_1^2 + 9 \left(g_2^4 - 2(h_b^2 + h_t^2)g_2^2 + 8h_b^2h_t^2 \right) \right) I(m_Q) + \\ &+ \frac{g_1^2}{3} (h_t^2 - \frac{g_1^2}{3}) I(m_U) + \frac{g_1^2}{6} (h_b^2 - \frac{g_1^2}{6}) I(m_D) + h_t^2h_b^2 I(m_U, m_D). \end{aligned} \quad (33)$$

$$-\Delta\lambda_4^f = (h_b^2 - \frac{g_2^2}{2}) (\frac{g_2^2}{2} - h_t^2) I(m_Q) - h_t^2h_b^2 I(m_U, m_D). \quad (34)$$

The three-dimensional integrals in (30)-(34) are

$$J(m_I) = \frac{1}{8\pi m_I}, \quad J(m_U, m_D) = \frac{1}{4\pi(m_U + m_D)}. \quad (35)$$

see (7), leading to series analogously to (12) and (17).

The logarithmic corrections for non-degenerate squark masses can be defined following [20] and [21]. Schematically, in the results of [15]) we replace $\ln \left(\frac{M_{SUSY}}{m_t^2} \right)$ by $\ln \left(\frac{m_Q m_U}{m_t^2} \right)$:

$$\Delta\lambda_1^{log} = -\frac{1}{384\pi^2} \left(11g_1^4 - 36h_b^2g_1^2 + 9 \left(g_2^4 - 4h_b^2g_2^2 + 16h_b^4 \right) \right) \ln \left(\frac{m_Q m_U}{m_t^2} \right), \quad (36)$$

$$\Delta\lambda_2^{log} = -\frac{1}{1536\pi^2} \left(44g_1^4 - 144h_t^2g_1^2 + 36g_2^4 + 576h_t^4 - 144g_2^2h_t^2 \right) \ln \left(\frac{m_Q m_U}{m_t^2} \right), \quad (37)$$

$$\Delta\lambda_3^{log} = -\frac{1}{384\pi^2} \left(-11g_1^4 + 18 \left(h_b^2 + h_t^2 \right) g_1^2 + \right. \quad (38)$$

$$\begin{aligned}
& +9 \left(g_2^4 - 2(h_b^2 + h_t^2) g_2^2 + 16h_b^2 h_t^2 \right) \ln \left(\frac{m_Q m_U}{m_t^2} \right), \\
\Delta \lambda_4^{log} &= \frac{3}{64\pi^2} \left(g_2^4 - 2(h_b^2 + h_t^2) g_2^2 + 8h_b^2 h_t^2 \right) \ln \left(\frac{m_Q m_U}{m_t^2} \right). \tag{39}
\end{aligned}$$

Large logarithms not connected with the renormalization group appear also in the wave-function renormalization yield, see below.

It is known that in order to renormalize the $\lambda\varphi^4$ theory, one needs to renormalize the self-coupling and the mass of the scalar field. If the $\lambda\varphi^4$ theory is supplemented by fermions with interactions defined by the Yukawa term, an additional wave-function renormalization is necessary. Similar situation takes place in the two-doublet model. Expanding the self-energy diagram (see the insertion to the leg in Fig.2, right) calculated with non-degenerate masses at finite temperature, we get at $p^2=0$ **the wave-function renormalization (w.f.r.) correction**, which is defined by a factor in front of p^2 . At zero temperature two ways of w.f.r. calculation can be used [22]. The following calculation is based on the integration of convergent w.f.r. contribution over the momentum squared, previously which has been used in differentiation. The standard subtraction scheme at zero momentum (BPSZ-scheme) in the divergent expression for the self-energy contribution, when the divergent pole part is subtracted, turns out to be not convenient at finite temperatures, because in summation over Matsubara frequencies not divergent integrals, but divergent series must be subtracted. Following [14] we can write

$$\begin{aligned}
\Delta \lambda_1^{wfr} &= \frac{1}{2}(g_1^2 + g_2^2)A'_{11}, & \Delta \lambda_2^{wfr} &= \frac{1}{2}(g_1^2 + g_2^2)A'_{22}, & (40) \\
\Delta \lambda_3^{wfr} &= -\frac{1}{4}(g_1^2 - g_2^2)(A'_{11} + A'_{22}), & \Delta \lambda_4^{wfr} &= -\frac{1}{2}g_2^2(A'_{11} + A'_{22}), & \Delta \lambda_5^{wfr} &= 0, \\
\Delta \lambda_6^{wfr} &= \frac{1}{8}(g_1^2 + g_2^2)(A'_{12} - A'_{21}^*) = 0, & \Delta \lambda_7^{wfr} &= \frac{1}{8}(g_1^2 + g_2^2)(A'_{21} - A'_{12}^*) = 0.
\end{aligned}$$

where A matrices 2×2 are ³

$$A'_{ij} = \left\{ \frac{2 \cdot 3h_U^2}{24\pi} F(m_Q^2, m_U^2, T) \begin{bmatrix} |\mu|^2 & -\mu^* A_U^* \\ -\mu A_U & |A_U|^2 \end{bmatrix} + (U \longrightarrow D, A \longleftrightarrow \mu) \right\} \left(1 - \frac{1}{2}l\right), \tag{41}$$

include the series (compare with Eq.(113) in [9], taking into account differentiation to get the finite w.f.r. yield)

$$\begin{aligned}
F(m_1^2, m_2^2, T) &= T \sum_{n=-\infty}^{+\infty} \frac{1}{(\sqrt{m_1^2 + (2\pi nT)^2} + \sqrt{m_2^2 + (2\pi nT)^2})^3} = \\
&= \frac{T}{(m_1 + m_2)^3} + 2T \sum_{n=1}^{+\infty} \frac{1}{(\sqrt{m_1^2 + (2\pi nT)^2} + \sqrt{m_2^2 + (2\pi nT)^2})^3}.
\end{aligned} \tag{42}$$

The sum of all w.f.r. corrections to $\lambda_{5,6,7}$ vanishes.

It is useful to check that the finite temperature corrections are reduced to the structures of zero-temperature MSSM, which play a role of **boundary condition at $T=0$** . Indeed in the limiting case of $T=0$ and degenerate squark mass parameters all equal to M_{SUSY} the threshold

³The equations in [14] are given for the general case of complex-valued μ , $A_{t,b}$.

corrections given by Eq.(23)-(29) are reduced to previous zero-temperature results [14, 23]. For example, let us take $\Delta\lambda_1$ for $m_a = m_b = M_{SUSY}$

$$\begin{aligned}\Delta\lambda_1 = & 3h_t^4|\mu|^4 I_2[M_{SUSY}] + 3h_b^4|A|^4 I_2[M_{SUSY}] + \\ & + h_t^2|\mu|^2 \left(\frac{g_1^2 - 3g_2^2}{2} I_1[M_{SUSY}] + 2g_1^2 I_1[M_{SUSY}] \right) + \\ & + h_b^2|A|^2 \left(\frac{12h_b^2 - g_1^2 - 3g_2^2}{2} I_1[M_{SUSY}] + (6h_b^2 - g_1^2) I_1[M_{SUSY}] \right),\end{aligned}\quad (43)$$

where the integrals are

$$I_1[M_{SUSY}] \equiv - \int \frac{d^4 k}{(2\pi)^4} \frac{1}{(k^2 + M_{SUSY}^2)^3} = - \frac{1}{16\pi^2} \frac{1}{2M_{SUSY}^2}, \quad (44)$$

$$I_2[M_{SUSY}] \equiv \int \frac{d^4 k}{(2\pi)^4} \frac{1}{(k^2 + M_{SUSY}^2)^4} = \frac{1}{16\pi^2} \frac{1}{6M_{SUSY}^4} \quad (45)$$

Transformation to Minkowski space leads to the change of sign in (44). The equality of the temperature series for $I_{1,2}$ to the symbolic expressions for the integrals can be numerically verified.

In the limiting case of $T=0$ and different squark mass parameters the reduction of (13) and (14) to the four-dimensional I_1 and I_2 can be achieved using

$$\frac{1}{[p^2 + m_a^2]^2 [p^2 + m_b^2]} = - \frac{1}{2m_a} \frac{\partial}{\partial m_a} \frac{1}{[p^2 + m_a^2] [p^2 + m_b^2]}, \quad (46)$$

Differentiating (46) with respect to m_b

$$\frac{1}{[p^2 + m_a^2]^2 [p^2 + m_b^2]^2} = - \frac{1}{2m_b} \frac{\partial}{\partial m_b} \frac{1}{[p^2 + m_a^2]^2 [p^2 + m_b^2]}. \quad (47)$$

then using Feynman parametrization (15), differentiation in the same way as in (46) and (47), and dimensional regularization to integrate over the four-momentum p with the following integration over the Feynman parameter, we arrive at

$$I_1 = - \int \frac{d^4 p}{(2\pi)^4} \frac{1}{[p^2 + m_a^2]^2 [p^2 + m_b^2]} = - \frac{m_a^2 - m_b^2 (1 + 2\ln \frac{m_a}{m_b})}{16\pi^2 (m_a^2 - m_b^2)^2}, \quad (48)$$

$$I_2 = \int \frac{d^4 p}{(2\pi)^4} \frac{1}{[p^2 + m_a^2]^2 [p^2 + m_b^2]^2} = \frac{m_a^2 - m_b^2 - (m_a^2 + m_b^2) \ln \frac{m_a}{m_b}}{8\pi^2 (m_a^2 - m_b^2)^3}. \quad (49)$$

In the limit $m_a = m_b$ these formulas coincide with the expressions for degenerate squark masses (44) and (45).

In calculations of the temperature dependent parameters $\lambda_i(T)$ of the effective MSSM potential at moderate temperatures truncated series with fifty terms (50 Matsubara frequencies) were used. Relative contributions of the remaining terms are less than 10^{-2} percent at $T=50$ GeV, decreasing with an increasing T . At small temperatures of the order of a few GeV an acceptable accuracy is achieved with 1000 terms. The effective parameters $\lambda_i(T)$ are less than one, justifying the perturbative approach, as a rule, at the squark mass parameters around several hundred GeV. However, strong parametric dependence is observed here, for example, at the squark mass parameters 200, 500 and 800 GeV the criteria $\lambda_i(T) < 1$ is valid up to $T \sim 860$ GeV, while taking degenerate squark masses at 600 GeV we found that at $T > 600$ GeV the perturbative regime cannot be used.

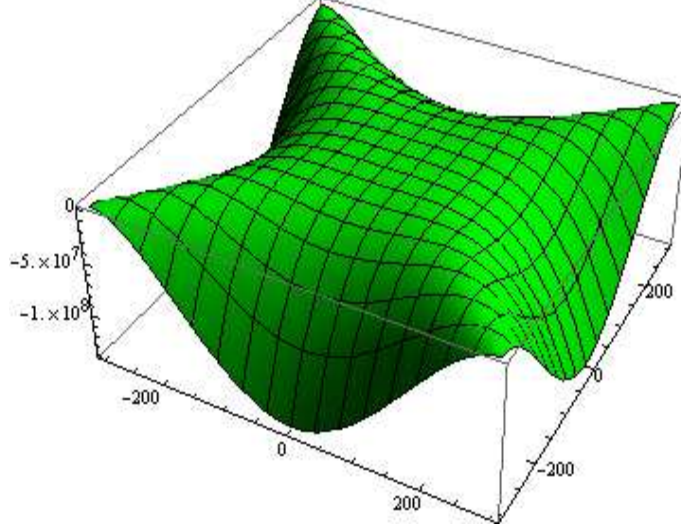


Figure 4: The zero-temperature surface of extrema for the two-doublet Higgs potential $U_0(v_1, v_2)$, see (2), at the scale M_{SUSY} .

3 Thermal evolution and the critical temperature

In view of the effective two-doublet potential structure defined by (2) one could assume that the two-dimensional picture of a broken symmetry of $U_{eff}(v_1, v_2)$ with a local minima at $T=0$, $v_{1,2} \neq 0$ appears in the sum of the potential terms with μ_1^2 , μ_2^2 and μ_{12}^2 of dimension 2 in the fields, which form a 'saddle' (a hyperboloid in the (v_1, v_2) space), and of the dimension 4 terms $\lambda_{1,...,7}$ which are increasing quartically, being unbounded from above. However, the situation is more involved because μ_1^2 , μ_2^2 , μ_{12}^2 and λ_i respect a number of constraints. In this section we are going to describe roughly some possible scenarios of temperature evolution in the effective two-doublet MSSM Higgs sector with threshold, logarithmic and wave-function renormalization one-loop corrections. Two sets of the squark mass parameters in the following numerical calculations are used

(A) $m_Q = 500$ GeV, $m_U = 200$ GeV, $m_D = 800$ GeV,

(B) $m_Q = 500$ GeV, $m_U = 800$ GeV, $m_D = 200$ GeV.

Masses of the third generation squarks are

$$m_{t_{1,2}}^2 = \frac{1}{2}((m_{t_L}^2 + m_{t_R}^2) \mp \sqrt{(m_{t_L}^2 - m_{t_R}^2)^2 + 4 A_1^2 m_{top}^2}),$$

$$m_{b_{1,2}}^2 = \frac{1}{2}((m_{b_L}^2 + m_{b_R}^2) \mp \sqrt{(m_{b_L}^2 - m_{b_R}^2)^2 + 4 A_2^2 m_b^2}),$$

where

$$m_{t_L}^2 = m_Q^2 + m_{top}^2 + \cos 2\beta m_Z^2 \left(\frac{1}{2} - \frac{2}{3} \sin^2 \theta_w \right),$$

$$m_{t_R}^2 = m_U^2 + m_{top}^2 + \cos 2\beta m_Z^2 \left(\frac{2}{3} \sin^2 \theta_w \right),$$

$$m_{b_L}^2 = m_Q^2 + m_b^2 + \cos 2\beta m_Z^2 \left(-\frac{1}{2} + \frac{1}{3} \sin^2 \theta_w \right),$$

$$m_{b_R}^2 = m_D^2 + m_b^2 + \cos 2\beta m_Z^2 \left(-\frac{1}{3} \sin^2 \theta_w \right)$$

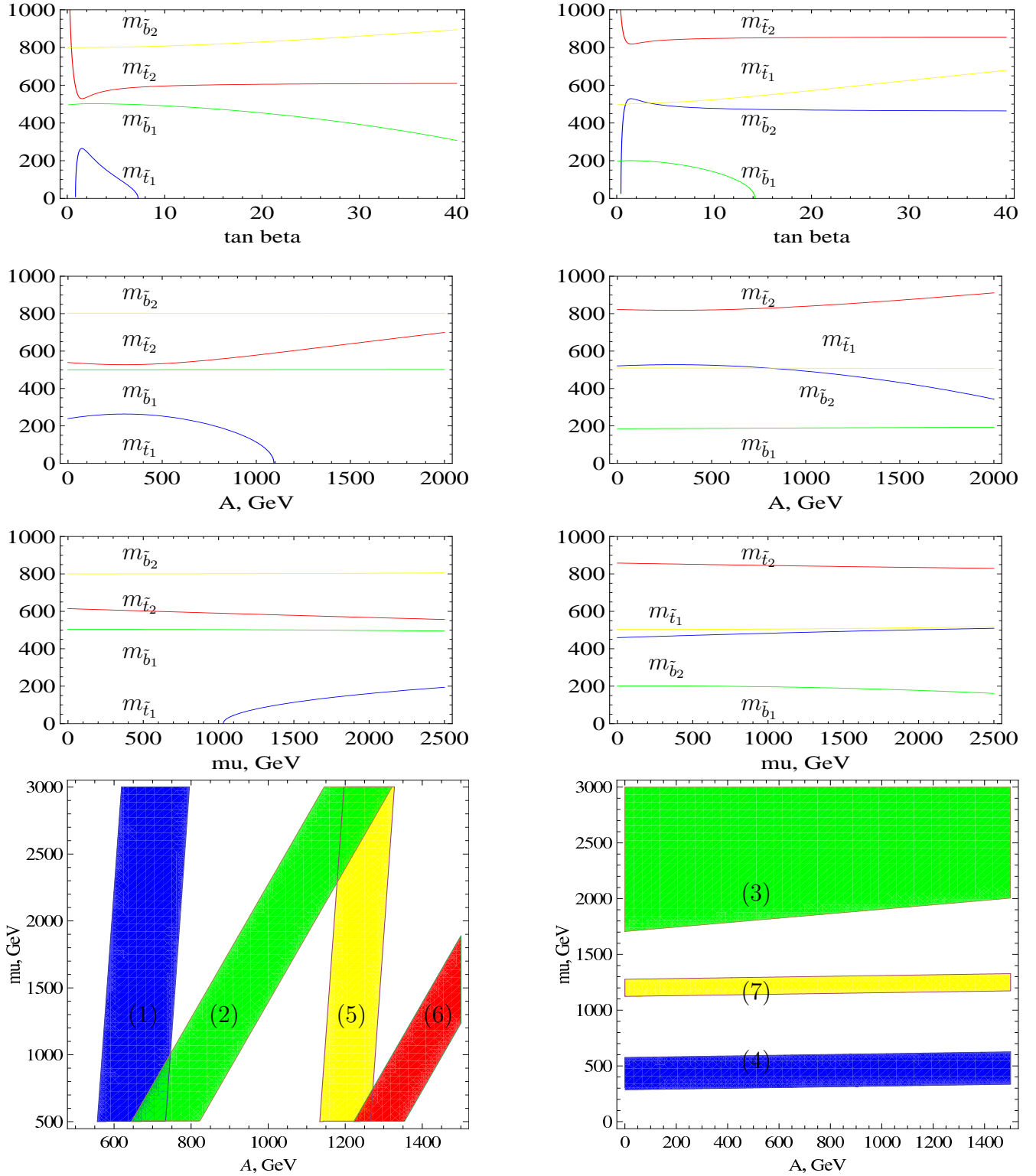


Figure 5: Third generation squark masses as a function of $\tan\beta$ (first row of plots), A (second row) and μ (third row of plots). For the left column of plots the squark sector parameter values are $m_Q = 500$ GeV, $m_U = 200$ GeV, $m_D = 800$ GeV, set (A). For the right column of plots the squark sector parameter values are $m_Q = 500$ GeV, $m_U = 800$ GeV, $m_D = 200$ GeV, set (B). The fourth row of plots demonstrates the regions of "light stop" $120 \text{ GeV} < m_{\tilde{t}_1} < 180 \text{ GeV}$ (left panel) and "light sbottom" $120 \text{ GeV} < m_{\tilde{b}_1} < 180 \text{ GeV}$ (right panel) in the (A, μ) plane. In the regions (1), $\tan\beta = 40$ and (2), $\tan\beta = 5$, squark parameters are given by set (A), in the region (3), where $\tan\beta = 5$, and (4), where $\tan\beta = 30$, squark parameters given by set (B). For regions (5) and (6) single parameter m_U of the set (A) is shifted to 400 GeV, for region (7) single parameter m_D of the set (B) is shifted to 400 GeV, other kept fixed.

and

$$A_1^2 = A_{t,b}^2 + \mu^2 \text{ctg}^2 \beta - 2 A_{t,b} \mu \text{ctg} \beta, \quad A_2^2 = A_{t,b}^2 + \mu^2 \text{tg}^2 \beta - 2 A_{t,b} \mu \text{tg} \beta.$$

With these parameters the third generation squark eigenstates $m_{\tilde{t}_{1,2}}$ and $m_{\tilde{b}_{1,2}}$ which masses are positively defined exist, as a rule, in an extensive regions of the $(\text{tg}\beta, A, \mu)$ parameter space, see Fig.5. Set (A) favors the light stop, while the light sbottom is a feature of the parameter set (B). Fixed parameters for the plots in Fig.5 are $\text{tg}\beta=5$, $A_{t,b}=1$ TeV, $\mu=1.5$ TeV, $m_{H^\pm}=180$ GeV. Squark masses vary in the range from 200 GeV to 800 GeV at the values of $A_{t,b}$ and μ up to the order of 1 TeV. Large difference of the stop masses is necessary to respect constraints following from the LEP2 experimental limit $m_h > 115$ GeV. The values of $\text{tg}\beta$ above 5 and large soft supersymmetry breaking parameters $A_{t,b}$ and μ of the order of m_Q also lead to an acceptable Higgs boson mass m_h (but weaken the strength of the electroweak phase transition if taken too large). At the same time substantial threshold corrections appear in the MSSM scenarios with large $A_{t,b}$ and μ , like the BGX scenario [24] and the CPX scenario [25], or the regions of MSSM parameter space close to BGX and CPX.

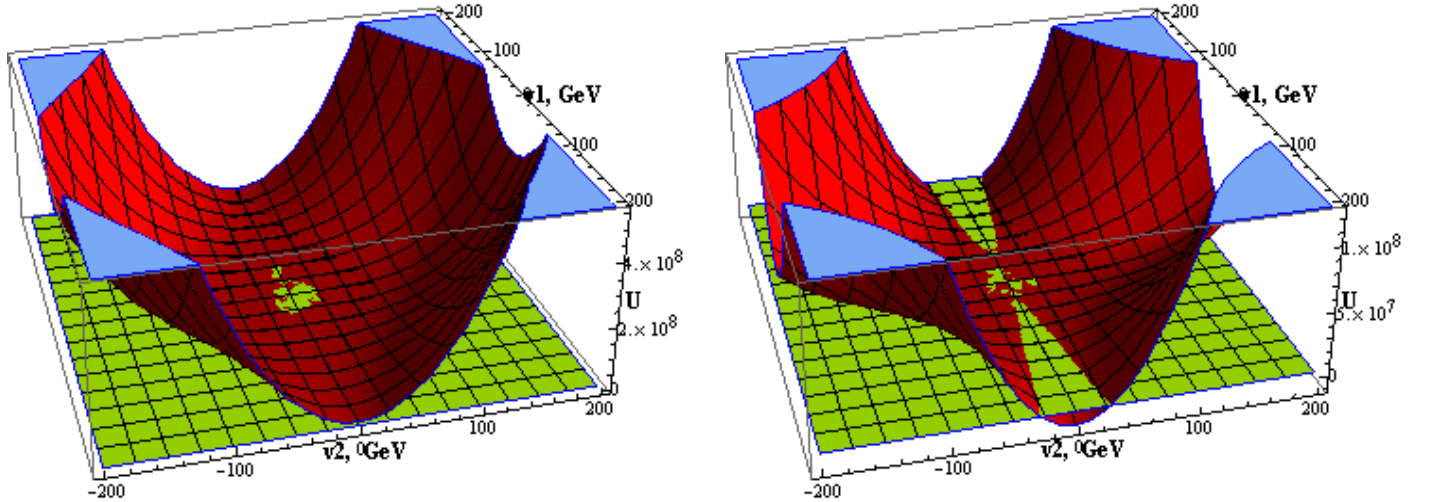


Figure 6: Development of the saddle configuration for the surface of stationary points of the potential $U_{eff}(v_1, v_2)$, see (2), at the critical temperature $T_c=120$ GeV. The squark sector parameter values are $m_Q=500$ GeV, $m_U=200$ GeV, $m_D=800$ GeV, $A_t=A_b=1200$ GeV, $\mu=500$ GeV, the charged Higgs boson mass $m_{H^\pm}=150$ GeV. Horizontal plane corresponds to $U_{eff}=0$.

In the following the equilibrium states of the effective potential (2) as a function of the two variables of state v_1 and v_2 and six temperature-dependent control parameters $\lambda_1(T), \dots, \lambda_7(T)$ are going to be analyzed. Local properties of $U_{eff}(v_1, v_2, \lambda_1, \dots, \lambda_7)$ are defined by a number of well-known theorems in the framework of the catastrophe theory (Morse and Thom theorems for the reduction of a potential function to the canonical form by a nonlinear transformation [26]). They describe properties of the stationary state $\nabla U_{eff}(v_1, v_2)=0$ defined by the stability matrix (also called the Hessian) $U_{ij} = \partial^2 U_{eff} / \partial v_i \partial v_j$. Simplest two-dimensional example of the Hessian is given by the MSSM Higgs potential at the SUSY scale, where $\lambda_1 = \lambda_2 = (g_1^2 + g_2^2)/8$, $\lambda_3 = (g_2^2 - g_1^2)/4$, $\lambda_4 = -g_2^2/2$ and $\lambda_5 = \lambda_6 = \lambda_7 = 0$ are independent of the temperature. The equilibrium matrix at the stationary points has the form

$$\left\| \begin{array}{cc} \frac{1}{4}(g_1^2 + g_2^2)v_1^2 + m_A^2 \frac{v_1^2}{v_1^2 + v_2^2} & -\frac{1}{4}(g_1^2 + g_2^2)v_1 v_2 - m_A^2 \frac{v_1 v_2}{v_1^2 + v_2^2} \\ -\frac{1}{4}(g_1^2 + g_2^2)v_1 v_2 - m_A^2 \frac{v_1 v_2}{v_1^2 + v_2^2} & \frac{1}{4}(g_1^2 + g_2^2)v_2^2 + m_A^2 \frac{v_2^2}{v_1^2 + v_2^2} \end{array} \right\| \quad (50)$$

(m_A is the CP-odd scalar mass) and the nonisolated (or degenerate) critical points defined by the condition $\det U_{ij} = 0$ lead to the equation $(g_1^2 + g_2^2)m_A^2(v_1^2 - v_2^2)^2/(v_1^2 + v_2^2) = 0$, so the MSSM surface of minima $U_0(v_1, v_2) = -(g_1^2 + g_2^2)(v_1^2 - v_2^2)^2/32$ is unbounded from below and the bifurcation set looks as the two 'flat directions' $v_1 = \pm v_2$, see Fig.4. Threshold corrections at zero temperature can be found in [23]. As a rule they transform the decreasing function in Fig.4 to a saddle configuration, slowly increasing along one of the 'flat directions' and more rapidly decreasing along the other.

In the general case the potential (2) as a function of the vacuum expectation values

$$U(v_1, v_2) = -\frac{\mu_1^2}{2}v_1^2 - \frac{\mu_2^2}{2}v_2^2 - \mu_{12}^2 v_1 v_2 + \frac{\lambda_1}{4}v_1^4 + \frac{\lambda_2}{4}v_2^4 + \frac{\lambda_{345}}{4}v_1^2 v_2^2 + \frac{\lambda_6}{2}v_1^3 v_2 + \frac{\lambda_7}{2}v_1 v_2^3 \quad (51)$$

includes temperature-dependent parameters $\lambda_i(T)$, $i=1, \dots, 7$, and $v_{1,2}(T)$, see Eq.(23)-(29), which define the thermal evolution from some high temperature T of the order of several hundred GeV down to zero. We denote $\lambda_{345} = \lambda_3 + \lambda_4 + \text{Re}\lambda_5$. Conditions of the extremum $\nabla U(v_1, v_2) = 0$ distinguishing an isolated (or nondegenerate) critical points

$$\mu_1^2 = \lambda_1 v_1^2 + (\lambda_3 + \lambda_4 + \text{Re}\lambda_5)\frac{v_2^2}{2} - \text{Re}\mu_{12}^2 \text{tg}\beta + \frac{v^2 s_\beta^2}{2}(3\text{Re}\lambda_6 \text{ctg}\beta + \text{Re}\lambda_7 \text{tg}\beta), \quad (52)$$

$$\mu_2^2 = \lambda_2 v_2^2 + (\lambda_3 + \lambda_4 + \text{Re}\lambda_5)\frac{v_1^2}{2} - \text{Re}\mu_{12}^2 \text{ctg}\beta + \frac{v^2 c_\beta^2}{2}(\text{Re}\lambda_6 \text{ctg}\beta + 3\text{Re}\lambda_7 \text{tg}\beta), \quad (53)$$

where

$$\text{Re}\mu_{12}^2 = \sin\beta \cos\beta [m_A^2 + \frac{v^2}{2}(2\text{Re}\lambda_5 + \text{Re}\lambda_6 \text{ctg}\beta + \text{Re}\lambda_7 \text{tg}\beta)],$$

are also mentioned as the minimization conditions which set to zero the linear terms in the physical fields h , H and A and ensure a local extremum at any point of the surface $U_{eff}(v_1, v_2)$ in the background fields space (see e.g. [14]) ⁴ Important input parameters of the two-doublet potential are $\text{tg}\beta = v_2/v_1$ and the charged Higgs boson mass

$$m_{H^\pm}^2 = m_W^2 + m_A^2 - \frac{v^2}{2}(\text{Re}\Delta\lambda_5 - \Delta\lambda_4) \quad (54)$$

where the effective temperature-dependent mass of the longitudinal W -boson is $m_{W_L}^2(v, T) = m_W^2(v) + \Pi_{W_L}(T)$, $\Pi_{W_L}(T) = 5g_2^2 T^2/2$ (with the one-loop Standard Model and third-generation squarks contributions included in the polarization operator; $m_W^2 = v^2 g_2^2/2$). If in the process of thermal evolution, when the system moves along some trajectory in the $v_1(T), v_2(T)$ plane, we require the minimization of U with respect to the scalar fields oscillation in the extremum $v_1(T), v_2(T)$ and continuously admit the interpretation of the system in terms of scalar states h, H and A , then μ_1^2 , μ_2^2 and μ_{12}^2 can be expressed by means of the effective parameters $\lambda_{1, \dots, 7}$ [14]. ⁵ Only μ_1^2 , μ_2^2 and μ_{12}^2 are dependent on the direction in the (v_1, v_2) plane, while $\lambda_{1, \dots, 7}$ are not.

First it is useful consider the simplified case $\lambda_6 = \lambda_7 = 0$. The two-doublet Higgs potential without λ_6 and λ_7 terms has been considered in the context of discrete Peccei-Quinn symmetry

⁴Although only the CP-conserving limit is considered, we keep the notation of real parts for the variables where a phase factor could appear in the general case.

⁵The normalization of $\lambda_{1,2}$ in [14] is different from [15] by a factor of 2

[27]. Nonisolated (or degenerate) critical points in the v_1, v_2 plane, defined by the condition $\det \partial^2 U / \partial v_i \partial v_j = 0$, or

$$\det \begin{vmatrix} 2\lambda_1 v_1^2 + \mu_{12}^2 \frac{v_2}{v_1} & -\mu_{12}^2 + \lambda_{345} v_1 v_2 \\ -\mu_{12}^2 + \lambda_{345} v_1 v_2 & 2\lambda_2 v_2^2 + \mu_{12}^2 \frac{v_1}{v_2} \end{vmatrix} = 0 \quad (55)$$

where the minimization conditions (52) and (53) (or, equivalently, the conditions for isolated points of $U(v_1, v_2)$) have been substituted. The system of two nonlinear equations for v_1, v_2

$$\begin{aligned} \lambda_1 v_1^3 + \frac{\lambda_{345}}{2} v_1 v_2^2 - \mu_1^2 v_1 - \mu_{12}^2 v_2 &= 0 \\ \lambda_2 v_2^3 + \frac{\lambda_{345}}{2} v_1^2 v_2 - \mu_2^2 v_2 - \mu_{12}^2 v_1 &= 0 \end{aligned} \quad (56)$$

can be factorized by the rotation in the v_1, v_2 plane

$$v_1 = \bar{v}_1 \cos \bar{\beta} - \bar{v}_2 \sin \bar{\beta}, \quad v_2 = \bar{v}_1 \sin \bar{\beta} + \bar{v}_2 \cos \bar{\beta} \quad (57)$$

where

$$\sin^2 \bar{\beta} = \frac{1}{2} \pm \frac{|\mu_1^2 - \mu_2^2|}{2\sqrt{(\mu_1^2 - \mu_2^2)^2 + 4\mu_{12}^4}}, \quad \cos^2 \bar{\beta} = \frac{1}{2} \mp \frac{|\mu_1^2 - \mu_2^2|}{2\sqrt{(\mu_1^2 - \mu_2^2)^2 + 4\mu_{12}^4}} \quad (58)$$

Then the factorized equations (56) are

$$\begin{aligned} \bar{v}_1 (\lambda_1 \bar{v}_1^2 + \frac{\lambda_{345}}{2} \bar{v}_2^2 - \bar{\mu}_1^2) &= 0 \\ \bar{v}_2 (\lambda_2 \bar{v}_2^2 + \frac{\lambda_{345}}{2} \bar{v}_1^2 - \bar{\mu}_2^2) &= 0 \end{aligned} \quad (59)$$

where

$$\bar{\mu}_{1,2}^2 = \frac{1}{2} (\mu_1^2 + \mu_2^2 \pm \sqrt{(\mu_1^2 - \mu_2^2)^2 + 4\mu_{12}^4}) \quad (60)$$

and the four types of bifurcation sets defined by the stability matrices $U_{ij}(v_1, v_2)$ can be easily found

$$\begin{aligned} (1) \quad & \lambda_1 \bar{v}_1^2 + \frac{\lambda_{345}}{2} \bar{v}_2^2 - \bar{\mu}_1^2 = 0 \text{ and } \lambda_2 \bar{v}_2^2 + \frac{\lambda_{345}}{2} \bar{v}_1^2 - \bar{\mu}_2^2 = 0, \quad U_{ij}(v_1, v_2) = \begin{vmatrix} 2\lambda_1 \bar{v}_1^2 & \lambda_{345} \bar{v}_1 \bar{v}_2 \\ \lambda_{345} \bar{v}_1 \bar{v}_2 & 2\lambda_2 \bar{v}_2^2 \end{vmatrix} \\ (2) \quad & \lambda_1 \bar{v}_1^2 - \bar{\mu}_1^2 = 0 \text{ and } \bar{v}_2 = 0, \quad U_{ij}(v_1, v_2) = \begin{vmatrix} 2\lambda_1 \bar{v}_1^2 & 0 \\ 0 & -\bar{\mu}_2^2 + \frac{\lambda_{345}}{2} \bar{v}_1^2 \end{vmatrix} \\ (3) \quad & \bar{v}_1 = 0 \text{ and } \lambda_2 \bar{v}_2^2 - \bar{\mu}_2^2 = 0, \quad U_{ij}(v_1, v_2) = \begin{vmatrix} -\bar{\mu}_1^2 + \frac{\lambda_{345}}{2} \bar{v}_2^2 & 0 \\ 0 & 2\lambda_2 \bar{v}_2^2 \end{vmatrix} \\ (4) \quad & \bar{v}_1 = 0 \text{ and } \bar{v}_2 = 0, \quad U_{ij}(v_1, v_2) = - \begin{vmatrix} \bar{\mu}_1^2 & 0 \\ 0 & \bar{\mu}_2^2 \end{vmatrix} \end{aligned}$$

Bifurcation set in the case (1) which is defined by $\det \partial^2 U / \partial v_i \partial v_j = 0$ can be understood in the elementary language. The surface of stationary points $U_{eff}(v_1, v_2) = -(\lambda_1 v_1^4 + \lambda_2 v_2^4 + \lambda_{345} v_1^2 v_2^2)/4$ is positively defined and unbounded from above if the Sylvester's criteria for the quadratic form $U_{eff}(v_1^2, v_2^2)$ is respected

$$\lambda_1 < 0, \quad \lambda_2 < 0, \quad \lambda_1 \lambda_2 - \frac{\lambda_{345}^2}{4} < 0 \quad (61)$$

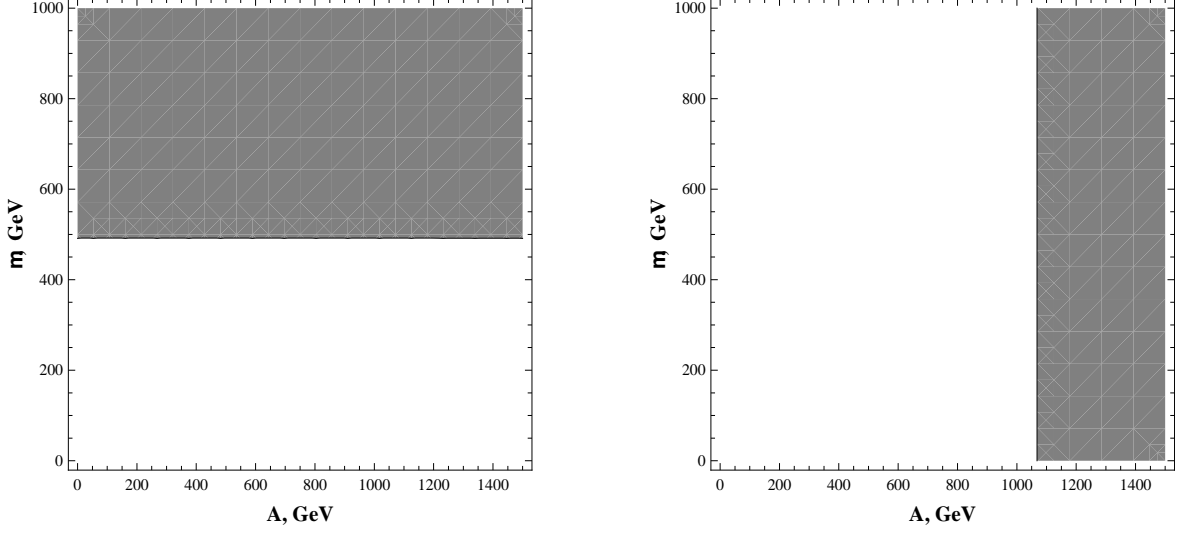


Figure 7: Contours of negatively defined λ_1 (left, dark grey area) and λ_2 (right, dark grey area) in the $(A_t = A_b, \mu)$ plane at the temperature 150 GeV, $m_{H^\pm} = 150$ GeV. Set (A), the case of light stop, is used for the squark sector parameter values ($m_Q = 500$ GeV, $m_U = 200$ GeV, $m_D = 800$ GeV).

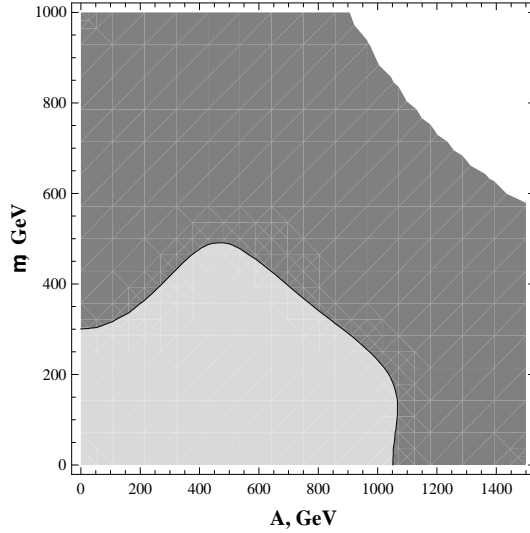


Figure 8: Contour of negatively defined determinant $\lambda_1 \lambda_2 - \lambda_{345}^2/4$ (dark grey area) in the $(A_t = A_b, \mu)$ plane at the temperature 150 GeV. Set (A), the case of light stop, is used for the squark sector parameter values ($m_Q = 500$ GeV, $m_U = 200$ GeV, $m_D = 800$ GeV).

At the critical temperature defined by the equation $\lambda_1 \lambda_2 - \lambda_{345}^2/4 = 0$ the positively defined potential surface of stationary points starts to develop the saddle configuration which is unbounded from below, see Fig.6. The "flat direction" at the critical temperature which is developed at the angle $\tan 2\theta = \lambda_{345}/(\lambda_1^2 - \lambda_2^2)$, or

$$\tan^2 \theta = \frac{\lambda_{345}^2}{(|\lambda_1 - \lambda_2| - \sqrt{(\lambda_1 - \lambda_2)^2 + \lambda_{345}^2})^2} \quad (62)$$

is defined by the control parameters $\lambda_1(T)$, $\lambda_2(T)$ and $\lambda_{345}(T)$ not depending on the v_1 and v_2 . The regions of positively and negatively defined λ_1 and λ_2 and the contour for Sylvester's criteria (61) are shown in Figs. 7 and 8 at the temperature $T = 150$ GeV in the $(A = A_t = A_b,$

μ) plane. The squark mass parameters m_Q , m_U and m_D are fixed as mentioned in the beginning of the section, set (A), the (A, μ) parameters are chosen in the vicinity of the contours which separate positively and negatively defined λ -parameters in (61). The critical temperature in this case is slightly above 120 GeV, insignificantly dependent on the values of $(A_{t,b}, \mu)$ if they are changing along the contours in Fig.7-8, separating the light grey and the dark grey areas. The

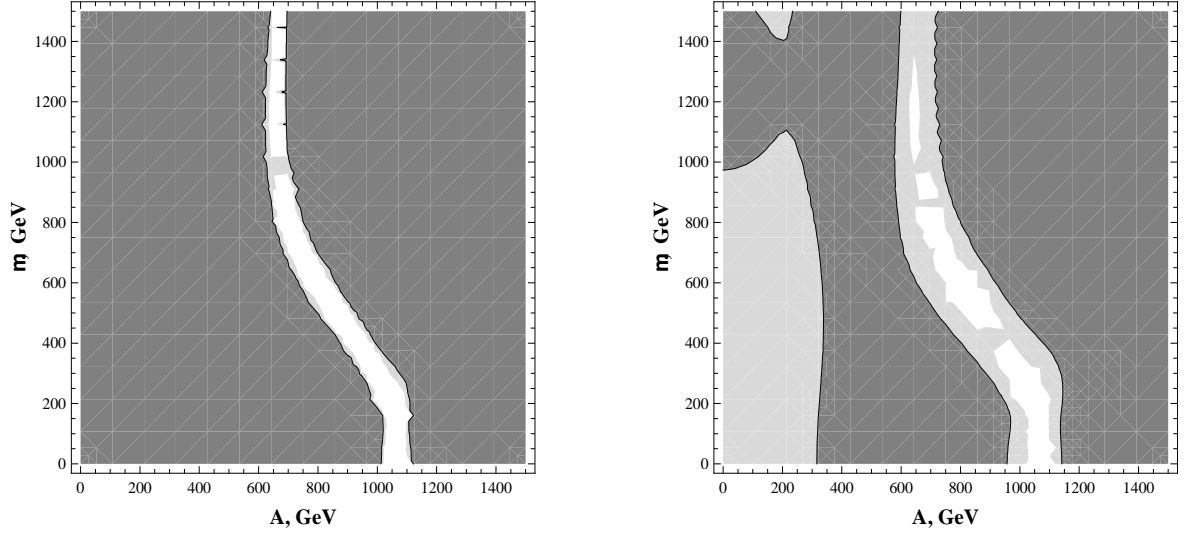


Figure 9: Contours for the criteria $\frac{v_c}{T_c} = 1$ in the $(A_t=A_b, \mu)$ plane. In the light grey regions $\frac{v_c}{T_c} > 1$. In order to include qualitatively the effect of E_{MSSM} , for the left plot $E = 2E_{SM}$ and for the right plot $E = 4E_{SM}$. $\lambda_6 = \lambda_7 = 0$, charged Higgs boson mass $m_{H^\pm} = 150$ GeV. Set (A), the case of light stop, is used for the squark sector parameter values ($m_Q = 500$ GeV, $m_U = 200$ GeV, $m_D = 800$ GeV).

strength of the electroweak phase transition along the direction (62) can be roughly estimated using the equation

$$\frac{v(T_c)}{T_c} = \frac{2\sqrt{2} E}{\lambda(\theta)} \quad (63)$$

where E is a temperature-independent factor in front of the cubic term $-ETv^3$ in the effective potential rewritten in the polar coordinates ($v = \sqrt{v_1^2 + v_2^2}$, $\theta = \arctan(v_2/v_1)$), and $\lambda(\theta)$ is a factor in front of the quartic term $v^4/4$. The cubic term is given by corrections coming from the resummation of the multiloop diagrams in the infrared region. In the case of a heavy stop which decouples [6], the effective potential is similar to Standard Model potential and

$$E_{SM} = \frac{2\sqrt{2}}{48\pi} [2g_2^3 + (g_1^2 + g_2^2)^{3/2}] = \frac{\sqrt{2}}{3} \frac{(2m_W^3 + m_Z^3)}{\pi v^3}. \quad (64)$$

In the case of a light stop one can use an approximation $E = E_{SM} + E_{MSSM}$, where an additional term [4]

$$E_{MSSM} = \frac{2\sqrt{2}}{3\pi v^3} m_t^3 \left(1 - \frac{\tilde{A}_t^2}{m_Q^2}\right)^{\frac{3}{2}}, \quad (65)$$

stop mixing parameter here $\tilde{A}_t = A_t - \mu/\mathbf{tg}\beta$. The quartic term along the direction (62) can be written in the form

$$\lambda(\theta) = -\frac{\lambda_1 + \lambda_{345}\mathbf{tg}^2\theta + \lambda_2\mathbf{tg}^4\theta + 2\lambda_6\mathbf{tg}\theta + 2\lambda_7\mathbf{tg}^3\theta}{(1 + \mathbf{tg}^2\theta)^2}. \quad (66)$$

The condition $v_c/T_c > 1$ [5], necessary to avoid sphaleron transitions which erase the baryon asymmetry initially generated at the electroweak phase transition, can be respected in a rather extensive regions of the (A, μ) plane. The contours of $v_c/T_c > 1$ in the (A, μ) plane (see Fig.9) separate the regions not only around the origin $(A, \mu) = (0, 0)$, but also the areas with (A, μ) of the order of 1 TeV, where the quartic term $\lambda(\theta)$ changes sign crossing zero along the flat direction (62).

If the set (B) is chosen for the squark mass parameters m_Q , m_U and m_D , corresponding to the case of light sbottom and relatively heavy stop, then the factor λ_2 is always positive in the broad range of temperatures from a few to a several thousands of GeV, the surface of stationary points is always a saddle, so the potential does not have a stable minimum at the origin $v_1 = v_2 = 0$.

For the general case of nonzero λ_6 and λ_7 defined by Eqs.(28) and (29) the effective potential $U_{eff}(v_1, v_2) = -(\lambda_1 v_1^4 + \lambda_2 v_2^4 + \lambda_{345} v_1^2 v_2^2 + 2\lambda_6 v_1^3 v_2 + 2\lambda_7 v_1 v_2^3)/4$ always demonstrates a saddle configuration for the surface of stationary points, which slopes become steeper with an increase of the temperature. Typical shape of $U_{eff}(v_1, v_2)$ is shown in Fig.10.

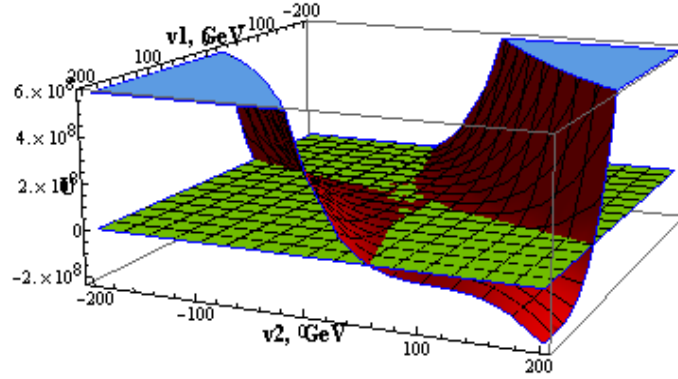


Figure 10: The surface of extrema for the potential $U_{eff}(v_1, v_2)$, see (2), with nonzero λ_6 and λ_7 at the temperature $T = 120$ GeV. The squark sector parameter values $m_Q = 500$ GeV, $m_U = 200$ GeV, $m_D = 800$ GeV, $A_t = A_b = 1500$ GeV, $\mu = 1000$ GeV, charged Higgs boson mass $m_{H^\pm} = 150$ GeV. Horizontal plane corresponds to $U_{eff} = 0$.

Bifurcation set in the cases (2) and (3) is different from the bifurcation set in the case (1). The condition $\bar{v}_1 = 0$ is equivalent to

$$|v_1 v_2 (\mu_1^2 - \mu_2^2)| = |\mu_{12}^2 (v_1^2 - v_2^2)| \quad (67)$$

so it follows from (58) that $\sin \bar{\beta} = v_1^2/v^2$ and $\cos \bar{\beta} = v_2^2/v^2$ (where $v^2 = v_1^2 + v_2^2$), so $\bar{v}_2^2 = v^2$. Then $\bar{\mu}_1^2 = (\mu_1^2 + \mu_2^2 + \mu_{12}^2 v^2/v_1 v_2)/2$. The factor $\bar{\lambda}_{345}$ in the potential with rotated vacuum expectation values $\bar{U}(\bar{v}_1, \bar{v}_2)$ can be found substituting (57) to (51)

$$\bar{\lambda}_{345} = \frac{1}{4}(6\lambda_1 c_\beta^2 s_\beta^2 + 6\lambda_2 c_\beta^2 s_\beta^2 + \lambda_{345}(s_\beta^4 - 4s_\beta^2 c_\beta^2 + c_\beta^4)) = (\lambda_1 + \lambda_2) \frac{3v_1^2 v_2^2}{2v^4} + \lambda_{345} \frac{v_1^4 + v_2^4 - 4v_1^2 v_2^2}{4v^4} \quad (68)$$

Using these equations one can rewrite the conditions for the case (2) $\bar{v}_1 = 0$ and $\bar{\mu}_1^2 = \bar{\lambda}_{345} \bar{v}_2^2/2$ in the form

$$(4\lambda_1 + \lambda_{345})v_1^4 + (4\lambda_2 + \lambda_{345})v_2^4 + (6\lambda_{345} - 2\lambda_1 - 2\lambda_2)v_1^2 v_2^2 = 0 \quad (69)$$

The regions of positively and negatively defined λ_1 and λ_2 and the contour for Sylvester's criteria for the form (69) are shown in Figs. 11 and 12 at the temperature $T = 150$ GeV in the $(A = A_t = A_b, \mu)$ plane. The squark mass parameters m_Q , m_U and m_D are fixed as mentioned in the beginning of the section, set (A), the (A, μ) parameters are chosen in the vicinity of the contours which separate positively and negatively defined λ -parameters in (69). As for the analysis of bifurcation set (1), set (B) again does not demonstrate a stable minimum at the origin for a broad range of temperatures.

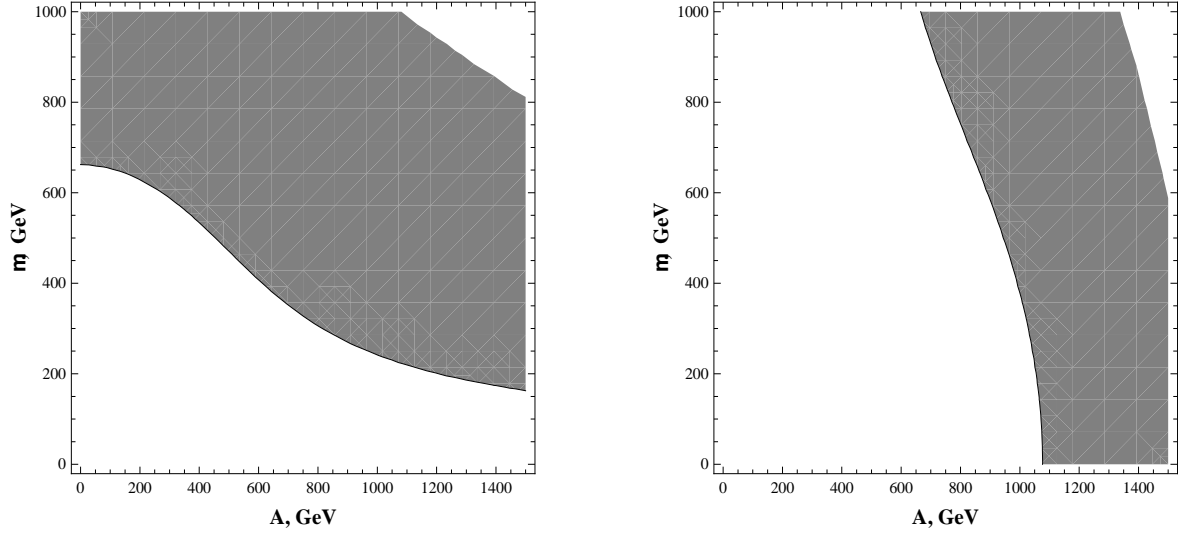


Figure 11: Contours of negatively defined $4\lambda_1 + \lambda_{345}$ (left, dark grey area) and $4\lambda_2 + \lambda_{345}$ (right, dark grey area) in the $(A_t = A_b, \mu)$ plane at the temperature 150 GeV, $m_{H^\pm} = 150$ GeV. Set (A), the case of light stop, is used for the squark sector parameter values ($m_Q = 500$ GeV, $m_U = 200$ GeV, $m_D = 800$ GeV).

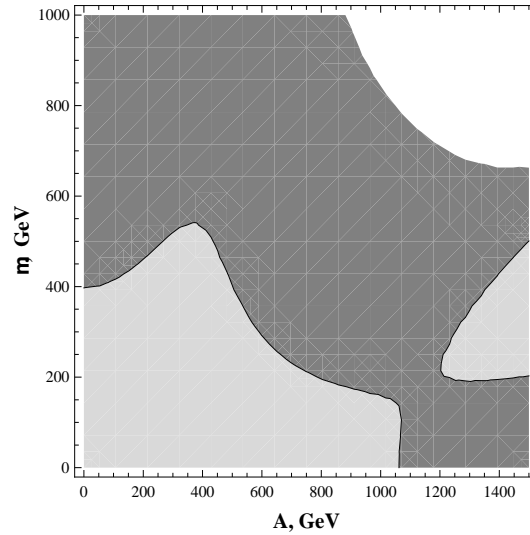


Figure 12: Contour of negatively defined determinant $(4\lambda_1 + \lambda_{345})(4\lambda_2 + \lambda_{345}) - (3\lambda_{345} - \lambda_1 - \lambda_2)^2$ (dark grey area) in the $(A_t = A_b, \mu)$ plane at the temperature 150 GeV. Set (A), the case of light stop, is used for the squark sector parameter values ($m_Q = 500$ GeV, $m_U = 200$ GeV, $m_D = 800$ GeV).

The phase transition for the case (2) is developed in the direction θ of the (v_1, v_2) plane

$$\text{tg}2\theta = \frac{3(3\lambda_{345} - \lambda_1 - \lambda_2)}{(4\lambda_1 + \lambda_{345})^2 - (4\lambda_2 + \lambda_{345})^2} \quad (70)$$

Bifurcation set in the case (4) $\bar{v}_1=0$ and $\bar{v}_2=0$ defined by the equation $\bar{\mu}_1^2\bar{\mu}_2^2=0$ can also be understood on the elementary level as a result of the diagonalization of the effective potential $U_{eff} = -\frac{\mu_1^2}{2}v_1^2 - \frac{\mu_2^2}{2}v_2^2 - \mu_{12}^2v_1^2v_2^2$ by the rotation (57), giving the form $U_{eff} = -\bar{\mu}_1^2\bar{v}_1^2 - \bar{\mu}_2^2\bar{v}_2^2$. This case is interesting not only in the case of an effective field theory under consideration but also in a more general physical framework. So far it has been assumed that we are in the framework of an effective field theory at the m_{top} energy scale, when the contributions from squarks decouple or a contribution of the potential terms with squarks (see the Appendix) is practically constant. However, if it is not the case and the Higgs bosons-squarks quartic term is positive definite with the global minimum at the origin $v_1 = v_2 = 0$, the phase transition may occur due to the development of a saddle configuration by the μ_1^2, μ_2^2 and μ_{12}^2 terms. Such situation may take place when the vacuum expectation values of charged and colored superpartners participate in the full MSSM scalar potential, possibly giving charge and color breaking minima [28]. For illustrative purposes it is convenient to use the polar coordinates $v_1(T) = v(T) \cos \bar{\beta}(T)$, $v_2(T) = v(T) \sin \bar{\beta}(T)$ for the vacuum expectation values. The mass term of the two-doublet potential has the form

$$U_{mass}(v, \bar{\beta}) = -\frac{v^2}{2}(\mu_1^2 \cos^2 \bar{\beta} + \mu_2^2 \sin^2 \bar{\beta}) - \frac{v^2}{2}\mu_{12}^2 \sin 2\bar{\beta} \quad (71)$$

By definition at the critical temperature the gradient of $U_{mass}(v, \bar{\beta})$ is zero along some direction in the (v_1, v_2) plane, then $\partial U_{mass}/\partial v = 0$ and $1/v \partial U_{mass}/\partial \bar{\beta} = 0$; it follows from these two equations

$$\text{tg}2\bar{\beta} = \frac{2\mu_{12}^2}{\mu_1^2 - \mu_2^2}, \quad (\mu_1^2\mu_2^2 - \mu_{12}^4)[(\mu_1^2 - \mu_2^2)^2 + 4\mu_{12}^4] = 0 \quad (72)$$

The first of these equations is equivalent to (58). The phase transition is characterized by the critical angle $\bar{\beta}(T)$ which defines the flat direction⁶ for the mass term at the temperature T_c in the background fields plane (v_1, v_2) , and at the real-valued μ_1 , μ_2 and μ_{12} the critical temperature is defined by the equation

$$\mu_1^2\mu_2^2 = \mu_{12}^4 \quad (73)$$

which is equivalent to $\bar{\mu}_1^2=0$ or $\bar{\mu}_2^2=0$. For a fixed set of the squark sector parameters⁷ the thermodynamical evolution of the effective potential is described by a $\nabla U_{eff}=0$ trajectory in the three-dimensional $(v, T, \text{tg}\beta)$ space, which is defined by the intersection of the two surfaces, corresponding to the equation (72) for the critical angle (" β -surface"), and the equation (73) for the μ_1 , μ_2 and μ_{12} (" μ -surface"). The cross sections of μ -surface (calculated without any approximations numerically) by the plane at fixed $T=0$, giving the $(v, \text{tg}\beta)$ contour, and the cross section at $\text{tg}\beta=1$ giving the (v, T) contour is shown in Fig.13. The presence of nonzero effective parameters λ_6 and λ_7 is essential to get the critical temperature of the order of 100 GeV.

⁶Flat directions may exist also in the quartic term separately taken, see e.g. [29].

⁷*Mathematica* package [30] with encoded representations of $\lambda_i(T)$ by means of series with $n=50$ was used to scan the MSSM parameter space. At low temperatures the convergence of Matsubara series becomes worse, so the number of terms up to $n=1000$ is needed to reach an acceptable accuracy.

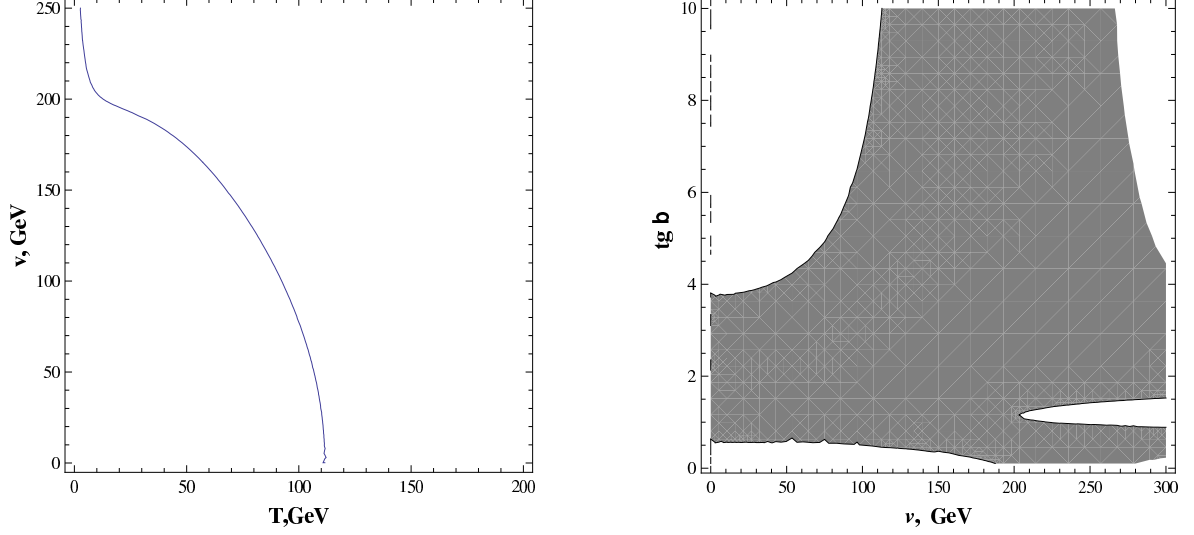


Figure 13: Cross sections of the μ -surface, see (72), at the temperature close to zero (right panel) and $\text{tg}\beta=1$ (left panel, see also Fig.1). White area in the right plot corresponds to the parameter values when the effective mass term (71) has a saddle configuration, $A_{t,b}=1800$ GeV, $\mu=2000$ GeV. The β -surface is very close to the μ -surface. The squark sector parameter values are $m_Q=500$ GeV, $m_U=200$ GeV, $m_D=800$ GeV, the charged Higgs boson mass $m_{H^\pm}=150$ GeV.

Useful analytical approximation can be obtained using the minimization conditions (52)-(53), then the critical angle $\bar{\beta}(T)$ defined by (72) can be expressed as ⁸

$$\text{tg}2\bar{\beta} = \text{tg}2\beta \frac{1}{\left(\frac{v^2}{2m_A^2} - \alpha_1\right)} \frac{1}{\frac{2\lambda_1 \cos^2 \beta - 2\lambda_2 \sin^2 \beta}{\cos 2\beta} - \lambda_{345} + \frac{2m_A^2}{v^2} + \alpha_2} \quad (74)$$

where

$$\alpha_1 = \frac{\lambda_5}{2} + \frac{1}{4}(\lambda_6 \text{ctg}\beta + \lambda_7 \text{tg}\beta), \quad \alpha_2 = \lambda_6(\text{tg}2\beta - \text{ctg}\beta) - \lambda_7(\text{tg}\beta + \text{tg}2\beta). \quad (75)$$

The assumption $\bar{\beta}(T) = \beta(0)$, i.e. only the modulo of $v(T)$ but not the direction in (v_1, v_2) plane are changed in the process of thermal evolution, gives for the critical angle (74)

$$-\frac{m_A^2}{v^2}(2\lambda_5 + \lambda_6 \text{ctg}\beta + \lambda_7 \text{tg}\beta) + \frac{v^2}{m_A^2} \left[\frac{2\lambda_1 - 2\lambda_2 \text{tg}^2 \beta + \lambda_6(3\text{tg}\beta - \text{ctg}\beta) + \lambda_7(\text{tg}^3 \beta - 3\text{tg}\beta)}{1 - \text{tg}^2 \beta} - \lambda_{345} \right] = 0. \quad (76)$$

This approximation may be too rough at small m_{H^\pm} , as pointed out in [6]. The saddle configuration changes not only the shape, but also the horizontal orientation in the process of thermal evolution. For the case $\lambda_5 = \lambda_6 = \lambda_7 = 0$ (76) is reduced to

$$\text{tg}^2 \beta = \frac{2\lambda_1 - \lambda_{345}}{2\lambda_2 - \lambda_{345}} \quad (77)$$

⁸In different context analogous relation between $\text{tg}\beta$ and $\text{tg}\bar{\beta}$ can be found in [6], where the mass term of the form $v^2 f(\beta, T)$ with $f(\beta, T) = a(\beta)T^2 - b(\beta)$ was analyzed for a special case of degenerate squark masses, $A = \mu = 0$ and within the high-temperature expansion. Our quartic potential is very different from the tree-level $(g_1^2 + g_2^2)/8 \lambda_T v^4 \cos^2 2\beta$ plus a logarithmic term [6], so the expression $3E/\lambda_T > 1$ of Bochkarev-Shaposhnikov criteria $v(T_c)/T_c > 1$ for the absence of sphaleron in the broken phase gives different results with nonzero threshold corrections.

Combining (53) and (76), where only the leading power terms in λ_i are kept and omitting $\lambda_5 \ll m_A^2/v^2$, the equation (73) can be written in the form

$$\lambda_1 (2\lambda_2 - \lambda_{345})^2 + \lambda_2 (2\lambda_1 - \lambda_{345})^2 + \lambda_{345} (2\lambda_1 - \lambda_{345})(2\lambda_2 - \lambda_{345}) = 0 \quad (78)$$

The vacuum expectation value v and mass m_A do not explicitly participate in this equation, only the dimensionless effective parameters λ_i of the quartic potential terms. The left-hand side of (78) approaches zero from below as v increases, demonstrating however no solution for the saddle configuration. This can be understood qualitatively if we rewrite (78) in the form $\lambda_1 \text{ctg}^2\beta + \lambda_2 \text{tg}^2\beta + \lambda_{345} = 0$ where the numerical values in the λ -pattern, see Fig.20, calculated in the BGX scenario $\lambda_1 < 0$, $\lambda_2 > 0$ and $\lambda_{345} < 0$, so in (77) $\text{tg}\beta < 1$.

Turning back to the case of effective field theory when the squarks decouple at the m_{top} energy scale, the evaluation of thermal masses of Higgs bosons, mixing angles and couplings can be done using results of [14]. For example, the thermal evolution of the CP-even Higgs bosons h and H is expressed by (compact notations $s_\alpha = \sin \alpha$, $c_\beta = \cos \beta$, etc. are used)

$$m_h^2 = c_{\alpha-\beta}^2 m_A^2 + v^2 (2\lambda_1 s_\alpha^2 c_\beta^2 + 2\lambda_2 c_\alpha^2 s_\beta^2 - 2(\lambda_3 + \lambda_4) c_\alpha c_\beta s_\alpha s_\beta + \text{Re}\lambda_5 (s_\alpha^2 s_\beta^2 + c_\alpha^2 c_\beta^2) - 2c_{\alpha+\beta} (\text{Re}\lambda_6 s_\alpha c_\beta - \text{Re}\lambda_7 c_\alpha s_\beta)), \quad (79)$$

$$m_H^2 = s_{\alpha-\beta}^2 m_A^2 + v^2 (2\lambda_1 c_\alpha^2 c_\beta^2 + 2\lambda_2 s_\alpha^2 s_\beta^2 + 2(\lambda_3 + \lambda_4) c_\alpha c_\beta s_\alpha s_\beta + \text{Re}\lambda_5 (c_\alpha^2 s_\beta^2 + s_\alpha^2 c_\beta^2) + 2s_{\alpha+\beta} (\text{Re}\lambda_6 c_\alpha c_\beta + \text{Re}\lambda_7 s_\alpha s_\beta)), \quad (80)$$

where the mixing angle α of the CP-even states h and H is

$$\text{tg}2\alpha = \frac{s_{2\beta} m_A^2 - v^2 ((\lambda_3 + \lambda_4) s_{2\beta} + 2c_\beta^2 \text{Re}\lambda_6 + 2s_\beta^2 \text{Re}\lambda_7)}{c_{2\beta} m_A^2 - v^2 (2\lambda_1 c_\beta^2 - 2\lambda_2 s_\beta^2 - \text{Re}\lambda_5 c_{2\beta} + (\text{Re}\lambda_6 - \text{Re}\lambda_7) s_{2\beta})}. \quad (81)$$

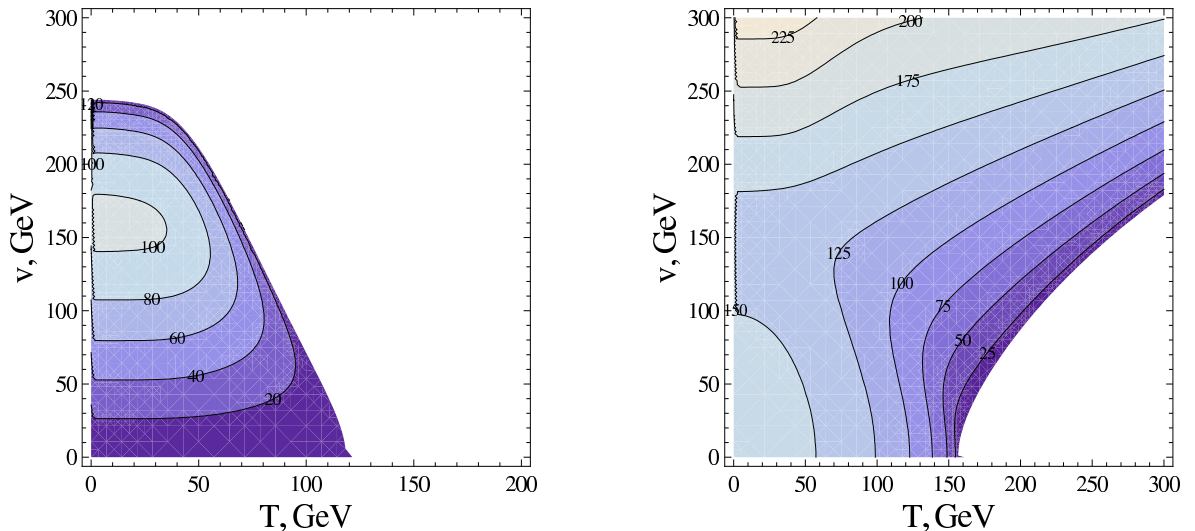


Figure 14: In the shaded areas m_h (left panel) and m_H (right panel) are positively defined at the parameter values $\text{tg}\beta=5$, $m_{H^\pm}=180$ GeV, $A_{t,b}=1200$ GeV, $\mu=500$ GeV. Isocontours of constant m_h and m_H masses are indicated. The squark sector parameter values are $m_Q=500$ GeV, $m_U=200$ GeV, $m_D=800$ GeV.

We show the regions of the (v,T) plane where the CP-even Higgs boson masses m_h and m_H are positively defined in Fig.14 - 16 (shaded areas). "Tachyonic" areas (shown in white

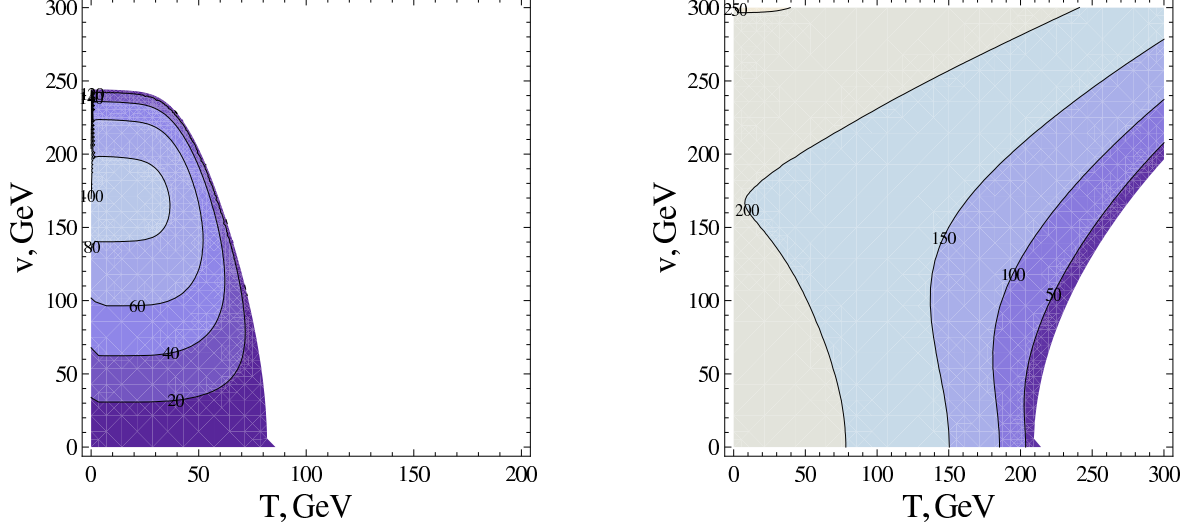


Figure 15: The same contours as in Fig.14 at $\tau g\beta = 15$, $m_{H^\pm} = 230$ GeV

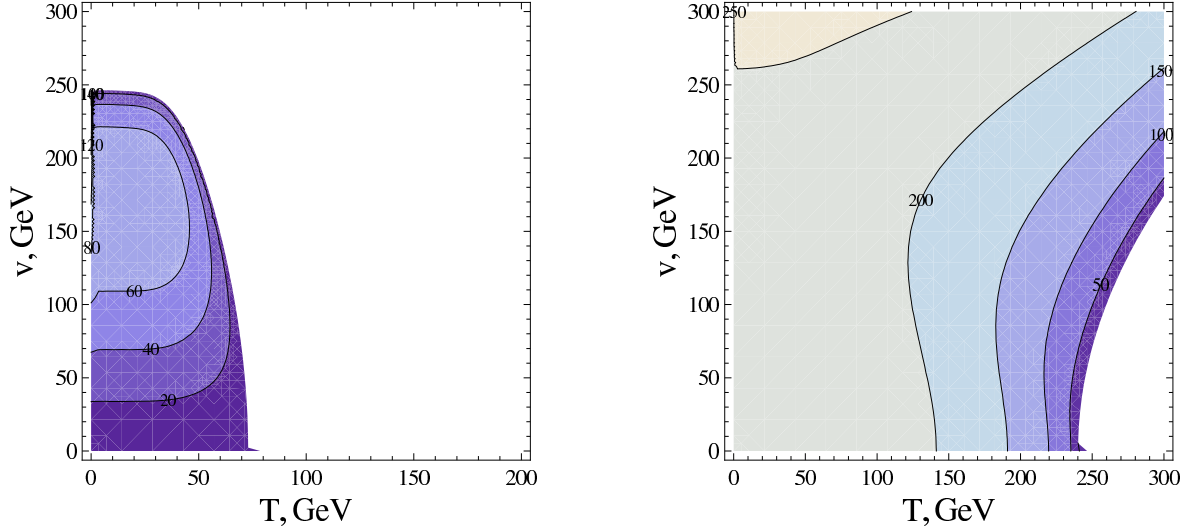


Figure 16: The same contours as in Fig.14 at $\tau g\beta = 40$, $m_{H^\pm} = 260$ GeV

colour) correspond to the negative squared masses of m_h or m_H , see (3), when the fluctuations of physical fields h and H near the unstable local extremum $(v_1(T), v_2(T))$ grow exponentially with time. Configuration of the effective potential $U_{eff}(h, H, A, T)$ expressed in the physical fields h, H in these areas is a saddle or a function with negative or indefinite sign values unbounded from below. The 'saddle' temperature $T_c = 120$ GeV (see Fig.6) is close to the temperature, when the thermal mass $m_h(T)$ vanishes, only at the low $\tau g\beta$ values. The heavy scalar mass $m_H(T)$ vanishes at the temperatures substantially higher than T_c . In the scenario under consideration at higher $\tau g\beta$ one should increase the charged scalar mass to respect the zero-temperature condition $v(0) = 246$ GeV.

4 Summary

Our analysis of the effective MSSM finite-temperature potential is based on a calculation of various one-loop temperature corrections from the squark-Higgs boson sector for the case of

nonzero trilinear parameters A_t , A_b and Higgs superfield parameter μ . Quantum corrections are incorporated in the parameters $\lambda_{1,\dots,7}(T)$ of the effective two-doublet potential (2), which is then explicitly rewritten in terms of Higgs boson mass eigenstates, using the approach developed in [14, 15]. The effective parameters $\lambda_1(T), \dots, \lambda_7(T)$ include the threshold corrections from triangle, box and "fish" diagrams together with the logarithmic and the wave-function renormalization terms. Dominant contribution comes from the triangle and box graphs (Fig.2, left and central) and can be written in a compact form by means of the generalized Hurwitz zeta-function.

Temperature evolution of the potential $U_{eff}(v_1, v_2)$ expressed in terms of the background fields $(v_1(T), v_2(T))$ is very sensitive to the MSSM scenario under consideration. We are using the scenarios with large $A_{t,b}$ and μ (about/of the order of 1 TeV), favored by the available experimental data. Two characteristic sets, (A) and (B) (see section 3), are used for the squark-Higgs boson sector parameters m_Q , m_U and m_D . A relatively light stop quark is inherent for the set (A), while with the set (B) sbottom quark is the lightest scalar quark eigenstate (see Fig. 5) for an extensive regions of the MSSM parameter space. Our analysis is essentially *two-dimensional*, i.e. the electroweak symmetry breaking is considered for the two-dimensional potential surface $U(v_1(T), v_2(T))$, the shape of which is defined by nine parameters $\mu_1^1, \mu_2^2, \mu_{12}^2$ and $\lambda_1, \dots, \lambda_7$ in the general (nonsupersymmetric) two-Higgs-doublet model. For the case of discrete Peccei-Quinn symmetry two parameters are equal to zero: $\lambda_6 = \lambda_7 = 0$. Using the terminology of the theory of catastrophes [26], we analyse the local behavior of the two-dimensional potential function, dependent on the several (less than five) control parameters. The surface of equilibrium points defined by the zero gradient $\nabla U(v_1, v_2) = 0$ looks like either a paraboloid function unbounded from above with the global minimum at the origin or a saddle configuration. Two types of surfaces are separated by the critical condition $\det \partial^2 U_{eff}(v_1, v_2) / \partial v_i \partial v_j = 0$ which defines the bifurcation set in the MSSM parameter space. The electroweak phase transition along some direction in the v_1, v_2 plane occurs when the temperature evolution of $\lambda_{1,\dots,5}$ from the TeV temperature scale down to zero temperature transforms a surface unbounded from above to a saddle configuration.

For example, the surface of equilibrium points with the two 'flat directions' $v_1 = \pm v_2$ for the tree-level MSSM potential at zero temperature is shown in Fig.4. When the non-temperature threshold corrections [23] to the tree-level zero temperature MSSM Higgs potential are included at some values of $A_{t,b}$ and μ , it changes the shape, becoming sign indefinite and unbounded from above, developing a saddle configuration.

In section 3 four types of bifurcation sets for the two-Higgs-doublet potential $U_{eff}(v_1, v_2)$ are found. The bifurcation set (1) defined by Eq.(61) develops a phase transition in the direction which is fixed by Eq.(62) in the (v_1, v_2) plane. In the MSSM only the parameter set (A) of the squark-Higgs bosons sector, characterized by the light stop quark, shows the necessary configuration of the surface for stationary points (paraboloid with a global minimum at the origin at high temperatures and a saddle at low temperatures⁹). The bifurcation contour (also called the separatrix in the catastrophe theory terminology) in the (A, μ) plane for the set (1) is shown in Fig.8. The parameter set (B) with the light sbottom always gives a saddle configuration because $\lambda_1 < 0$ and $\lambda_2 > 0$ in the parameter space. The bifurcation sets (2) and (3) are similar, demonstrating a phase transition in the direction defined by Eq.(70) in the (v_1, v_2) plane. The bifurcation contours in the (A, μ) plane for the set (2) are shown in Fig.12. Again, only the parameter set (A) with the light stop demonstrates the necessary configuration of the

⁹The LHC exclusion contours [31] for the gluino, squark and wino masees based on the luminosity 35 pb^{-1} at $\sqrt{s} = 7 \text{ TeV}$ in the GMSB and mSUGRA scenarios have yet no significant impact on the full MSSM parameter space, but reduce a parametric configurations to some extent.

equilibrium surfaces. The bifurcation set (4) includes a phase transition in the direction of Eq.(72) at the temperature defined by Eq.(73). This case was analyzed earlier in the literature in the context of the one-dimensional effective potential. The bifurcation contours for the case of parameter set (A) are shown in Fig. 13. Summarizing, in all four cases the global minimum at the origin $v_1 = v_2 = 0$, $U_{eff}(0, 0) = 0$ at high temperatures is transformed to a local minimum with $U_{eff}(v_1, v_2) < 0$ at a lower temperature for the parameter set (A), but the directions of transition to this minimum in the (v_1, v_2) plane are different.

Oscillations of Higgs fields in the vicinity of an extremum $(v_1(T), v_2(T))$ give the effective potential with a minimum moving along the surface of stationary points. The potential $U_{eff}(h, H, A)$ written in terms of physical Higgs fields (i.e. Higgs mass eigenstates h, H and A) demonstrates the spectrum of scalars with positively defined masses which are reaching zero at different temperatures, see Figs.14 - 16. These temperatures are, as a rule, not close to the 'critical' temperature T_c , when the potential $U_{eff}(v_1, v_2)$ forms a horizontal 'narrow gully', so not only the first, but also the second derivatives are zero in some direction.

The isocontours for CP-even scalar masses m_h and m_H fall down in an extremely narrow temperature region near $T = 0$, see Figs.14 - 16, so during the 'overturn' of the potential a nearly step-like decrease of $v(T)$ must happen to keep constant masses.

Although our evaluation is performed at the one-loop only and not all possible corrections are considered, usually it is possible to adjust μ , $A_{t,b}$ (or $X_{t,b}$), m_Q , m_U and m_D of the MSSM parameter space in such a way that the boundary condition for zero temperature $v(0) = 246$ GeV is respected, the lightest Higgs boson mass is large enough, the critical temperature is of the order of 100 GeV or higher, and the phase transition is of the first order. Threshold corrections with μ , $A_{t,b}$ of the order of 1 TeV can increase the strength the electroweak phase transition. Independently on the temperature evolution scenarios, one should not forget that the value of $\tan\beta$ at zero temperature must be consistent with the range from 5 to 50-60, provided by phenomenological restrictions from LEP2 and Tevatron data for the reactions $e^+e^- \rightarrow hZ$, $h \rightarrow b\bar{b}$, and $pp \rightarrow t\bar{t}$, $t \rightarrow H^\pm b$. In the nearest future useful information about the allowed regions of the MSSM parameter space could be provided by the LHC Higgs physics program [32]. Availability of the criteria $v(T_c)/T_c \sim 1$ for the absence of sphaleron in the broken phase deserves a more careful study with more precise evaluation of radiative corrections from other sources, especially the infrared ones.

Only the case of real-valued MSSM parameters $A_{t,b}$ and μ was considered. Generalization to the complex-valued parameters (the case of explicit CP violation in the squark-Higgs and the two-doublet Higgs sectors) is straightforward with radiation corrections defined by Eqs.(27)-(29), where phases of $A_{t,b}$ and μ can be introduced. Complex $\lambda_{5,6,7}$ lead to the mixing of CP-even h, H and CP-odd A scalars resulting in the Higgs bosons without a definite CP-parity h_1, h_2 and h_3 with specific properties, modifying the qualitative picture described above.

Acknowledgements

M.D.(MSU) is grateful to Mikhail Shaposhnikov for useful discussion. Work was partially supported by grants ADTP 3341, RFBR 10-02-00525-a, NS 1456.2008.2 and FAP contract 5163.

5 Appendix

Inputs and some details of various quantum corrections calculation, see Eq.(23) and the following formulas, are given below. Supersymmetric potential of the Higgs bosons - third generation of scalar quarks interaction has the form [20]

$$\mathcal{V}^0 = \mathcal{V}_M + \mathcal{V}_\Gamma + \mathcal{V}_\Lambda + \mathcal{V}_{\tilde{Q}}, \quad (82)$$

where

$$\mathcal{V}_M = -\mu_{ij}^2 \Phi_i^\dagger \Phi_j + M_Q^2 (\tilde{Q}^\dagger \tilde{Q}) + M_{\tilde{U}}^2 \tilde{U}^* \tilde{U} + M_{\tilde{D}}^2 \tilde{D}^* \tilde{D}, \quad (83)$$

$$\mathcal{V}_\Gamma = \Gamma_i^D (\Phi_i^\dagger \tilde{Q}) \tilde{D} + \Gamma_i^U (i\Phi_i^T \sigma_2 \tilde{Q}) \tilde{U} + \Gamma_i^{D*} (\tilde{Q}^\dagger \Phi_i) \tilde{D}^* - \Gamma_i^{U*} (i\tilde{Q}^\dagger \sigma_2 \Phi_i^*) \tilde{U}^*, \quad (84)$$

$$\begin{aligned} \mathcal{V}_\Lambda = & \Lambda_{ik}^{jl} (\Phi_i^\dagger \Phi_j) (\Phi_k^\dagger \Phi_l) + (\Phi_i^\dagger \Phi_j) [\Lambda_{ij}^Q (\tilde{Q}^\dagger \tilde{Q}) + \Lambda_{ij}^U \tilde{U}^* \tilde{U} + \Lambda_{ij}^D \tilde{D}^* \tilde{D}] + \\ & + \bar{\Lambda}_{ij}^Q (\Phi_i^\dagger \tilde{Q}) (\tilde{Q}^\dagger \Phi_j) + \frac{1}{2} [\Lambda \epsilon_{ij} (i\Phi_i^T \sigma_2 \Phi_j) \tilde{D}^* \tilde{U} + \text{h.c.}] , \quad i, j, k, l = 1, 2, \end{aligned} \quad (85)$$

$\mathcal{V}_{\tilde{Q}}$ denotes the four scalar quarks interaction terms, $\sigma_2 \equiv \begin{pmatrix} 0 & i \\ -i & 0 \end{pmatrix}$, and Λ^I are defined by the tree-level equalities

$$\begin{aligned} \Lambda^Q &= \text{diag}\left\{\frac{1}{4}(g_2^2 - g_1^2 Y_Q), \quad h_U^2 - \frac{1}{4}(g_2^2 - g_1^2 Y_Q)\right\}, \\ \bar{\Lambda}^Q &= \text{diag}\left\{h_D^2 - \frac{1}{2}g_2^2, \frac{1}{2}g_2^2 - h_U^2\right\}, \quad \Lambda^U = \text{diag}\left\{-\frac{1}{4}g_1^2 Y_U, h_U^2 + \frac{1}{4}g_1^2 Y_U\right\}, \\ \Lambda^D &= \text{diag}\left\{h_D^2 - \frac{1}{4}g_1^2 Y_D, \frac{1}{4}g_1^2 Y_D\right\}, \quad \Lambda = -h_U h_D. \end{aligned}$$

Here the squark hypercharges are $Y_{Q_i} = 1/3(-1)$, $Y_{D_i} = 2/3(2)$, $Y_{U_i} = -4/3$, and the Yukawa couplings for the third generation squarks $h_t = \frac{\sqrt{2}m_t}{v \sin \beta}$, $h_b = \frac{\sqrt{2}m_b}{v \cos \beta}$. In the general case of complex-valued parameters

$$\Gamma_{\{1;2\}}^U = h_U \{-\mu^*; A_U\}, \quad \Gamma_{\{1;2\}}^D = h_D \{A_D; -\mu^*\}, \quad (86)$$

In order to calculate, e.g., the one-loop threshold corrections (23)-(29) first we extract from the potential (82) the triple and quartic interactions presented in Fig.17 and Fig.18. The triangle and box diagrams which contribute, for example, to the threshold corrections included in λ_1 are shown in Fig.19 together with symbolic expressions for the temperature one-loop integrals. Their sum multiplied by the color factor 3 gives λ_1^{thr} , see (23).

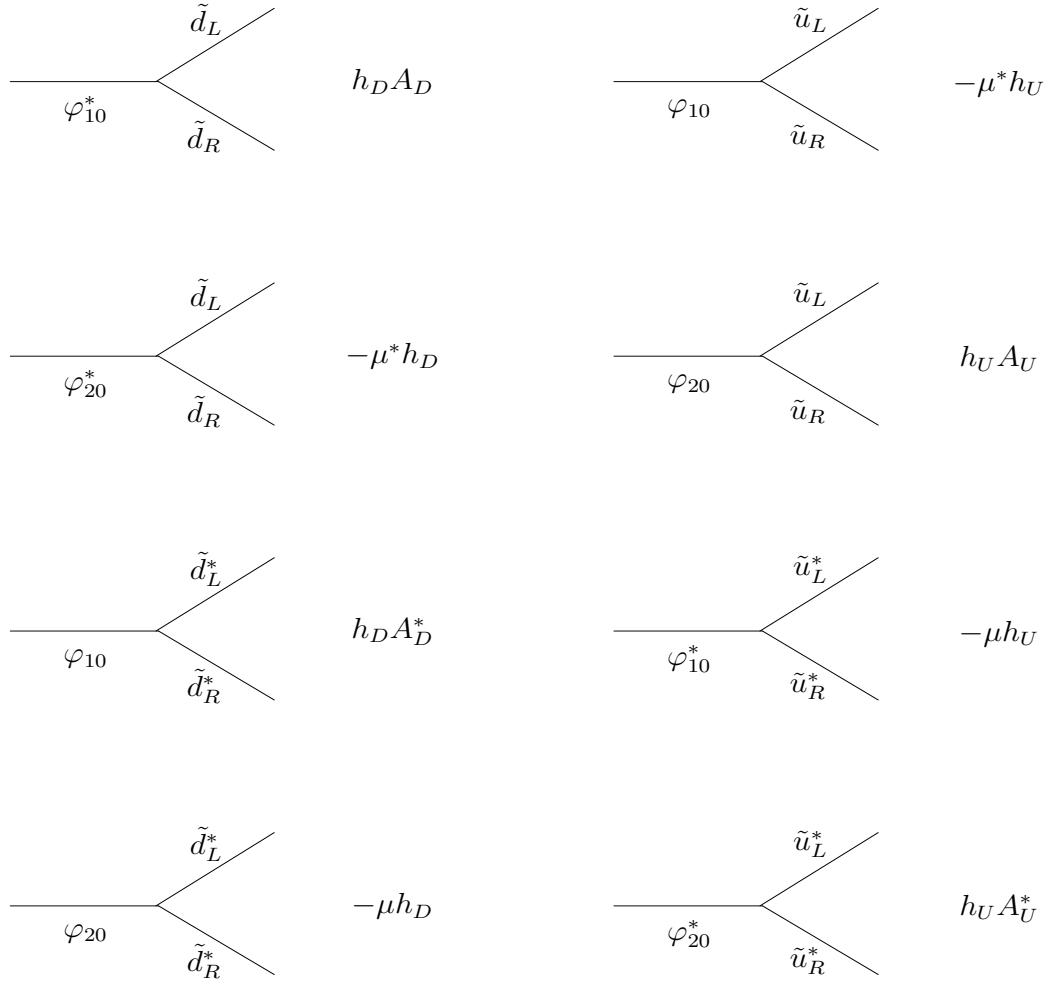


Figure 17: The triple interactions extracted from the squark-Higgs sector, see (82).

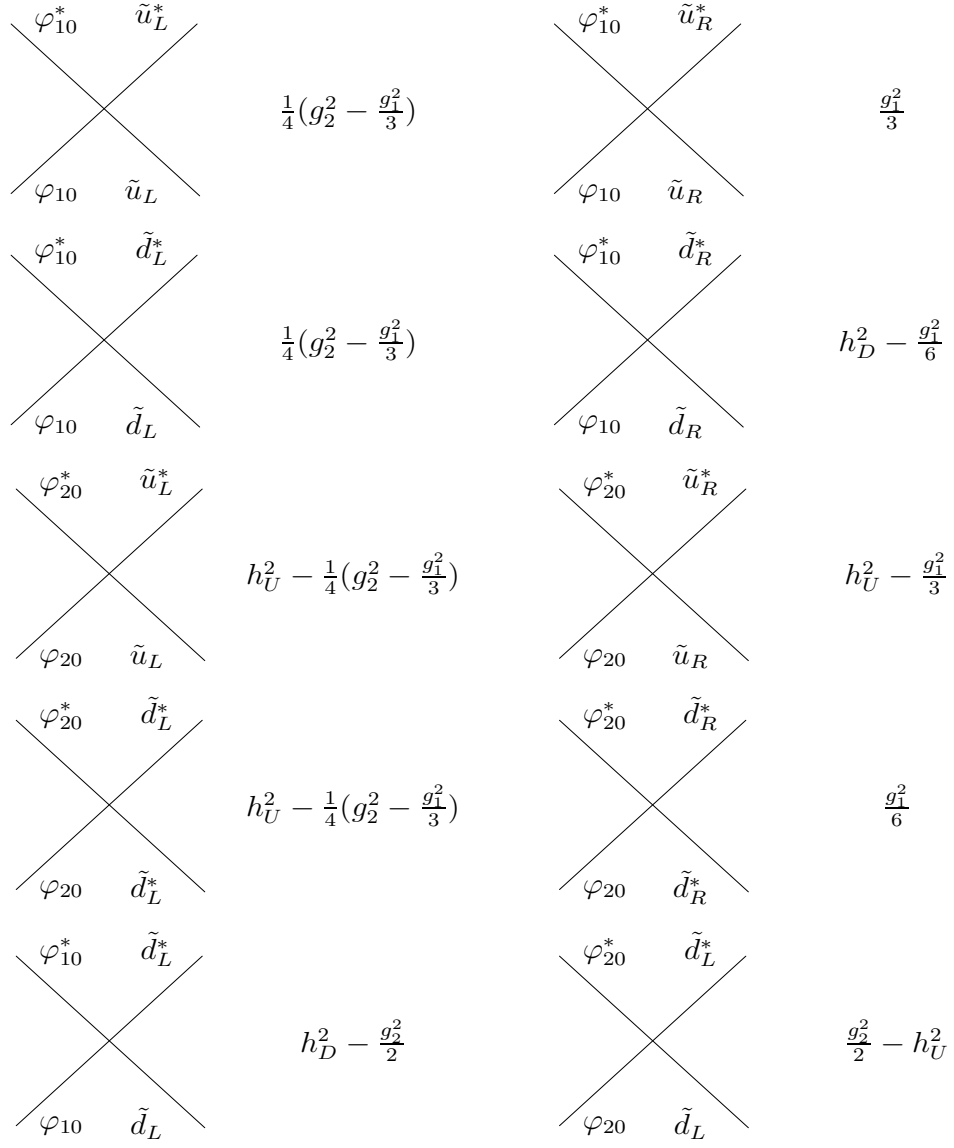


Figure 18: The quartic interactions extracted from the squark-Higgs sector, see (82).

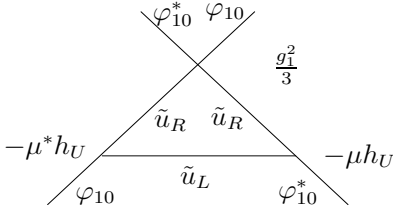
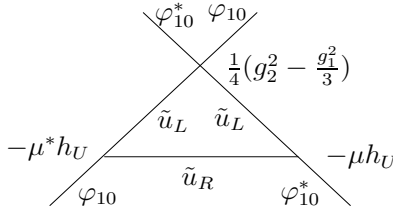
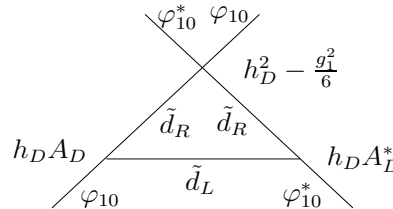
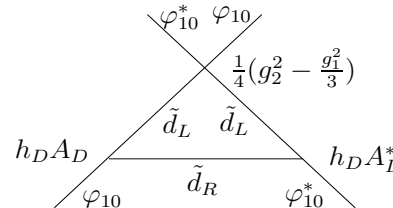
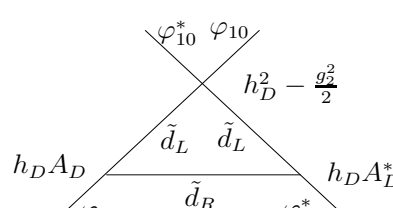
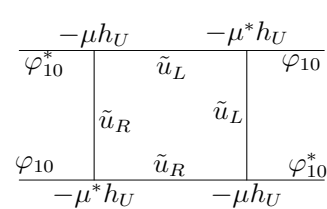
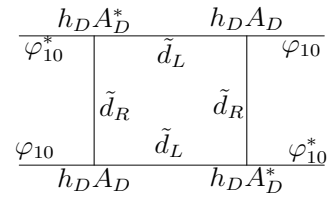
	$2\frac{g_1^2}{3}h_U^2 \mu ^2I_1(m_U, m_Q)$
	$2\frac{1}{4}(g_2^2 - \frac{g_1^2}{3})h_U^2 \mu ^2I_1(m_Q, m_U)$
	$2(h_D^2 - \frac{g_1^2}{6})h_D^2 A_D ^2I_1(m_D, m_Q)$
	$2\frac{1}{4}(g_2^2 - \frac{g_1^2}{3})h_D^2 A_D ^2I_1(m_Q, m_D)$
	$2(h_D^2 - \frac{g_2^2}{2})h_D^2 A_D ^2I_1(m_Q, m_D)$
	$ \mu ^4 h_U^4 I_2(m_Q, m_U)$
	$h_D^4 A_D ^4 I_2(m_Q, m_D)$

Figure 19: Triangle and box diagrams contributing to λ_1^{thr} , see (23).

References

- [1] for a review, see: V.A. Rubakov, M.E. Shaposhnikov, *Usp.Fiz.Nauk* **166** (1996) 493 (hep-ph/9603208)
A.G. Cohen, D.B. Kaplan, A.E. Nelson, *Ann.Rev.Nucl.Part.Sci.* **43** (1993) 27 (hep-ph/9302210)
A.D. Dolgov, *Phys.Rep.* **222** (1992) 309
- [2] A. Linde, *Rep.Prog.Phys.* **42** (1979) 389
D. Kirzhnits, A. Linde, *Ann.Phys.* **101** (1976) 195
S. Weinberg, *Phys.Rev. D* **9** (1974) 3357
L. Dolan, R. Jackiw, *Phys.Rev. D* **9** (1974) 3320
- [3] L. Fromme, S. Huber, M. Seniuch, *JHEP* 0611 (2006) 038 (hep-ph/0605242)
Y. Okada et al., in: *Proc. of CERN Workshop on CP studies and nonstandard Higgs physics*, ed. by S.Kraml, G.Azuelos, D.Dominici, J.Ellis, G.Grenier, H.Haber, J.S.Lee, D.Miller, A.Pilaftsis, W.Porod, CERN Yellow Report 2006–009, 2006 (hep-ph/0608079)
K. Funakubo, S. Tao, F. Toyoda, *Prog.Theor.Phys.* **109** (2003) 415 (hep-ph/0211238)
M. Losada, *Nucl. Phys. B* **569** (2000) 125 (hep-ph/9905441)
M. Laine, K. Rummukainen, *Nucl.Phys. B* **545** (1999) 141 (hep-ph/9811369)
M. Brhlik, G.J. Good, G.L. Kane, *Phys.Rev. D* **63** (2001) 035002 (hep-ph/9911243)
J. Cline, K. Kainulainen, *Nucl.Phys. B* **510** (1998) 88 (hep-ph/9705201)
P. Arnold, O. Espinosa, *Phys.Rev. D* **47** (1993) 3546 (Erratum-ibid. D50 (1994) 6662) (hep-ph/9212235)
G.F. Giudice, *Phys.Rev. D* **45** (1992) 3177
N. Turok, J. Zadrozny, *Nucl. Phys. B* **369** (1992) 729
A.I. Bochkarev, S.V. Kuzmin, M.E. Shaposhnikov, *Phys.Lett. B* **244** (1990) 275
- [4] M. Carena, G. Nardini, M. Quiros, C.E.M. Wagner. *Nucl.Phys. B* **812** (2009) 243 (arXiv:0809.3760 [hep-ph])
M. Carena, G. Nardini, M. Quiros and C.E.M. Wagner, *JHEP* 10 (2008) 062 (arXiv:0806.4297 [hep-ph])
M. Carena, M. Quiros, C.E.M. Wagner, *Phys.Lett. B* **380** (1996) 81 (hep-ph/9603420)
- [5] A.I. Bochkarev, M.E.Shaposhnikov, *Mod.Phys.Lett. A* **2** (1987) 417
M.E. Shaposhnikov, *JETP Lett.* **44** (1986) 465
- [6] A. Brignole, J.R. Espinosa, M. Quiros, F. Zwirner, *Phys. Lett. B* **324** (1994) 181 (hep-ph/9312296)
- [7] K. Kajantie, M. Laine, K. Rummukainen, M. Shaposhnikov, *Nucl.Phys. B* **466** (1996) 189 (hep-lat/9510020)
K. Kajantie, K. Rummukainen, M. Shaposhnikov, *Nucl.Phys. B* **407** (1993) 356 (hep-ph/9305345)
- [8] D. Gross, R. Pisarski, L. Yaffe, *Rev.Mod.Phys.* **53** (1981) 43
A. Linde, *Phys.Lett. B* **96** (1980) 289
- [9] K. Kajantie, M. Laine, K. Rummukainen, M. Shaposhnikov, *Nucl.Phys. B* **458** (1996) 90 (hep-ph/9508379)

- K. Farakos, K. Kajantie, K. Rummukainen, M. Shaposhnikov, Nucl.Phys. B**425** (1994) 67 (hep-ph/9404201)
- [10] A. Jakovac, K. Kajantie, A. Patkos, Phys.Rev. D**49** (1994) 6810
S. Nadkarni, Phys.Rev. D**27** (1983) 917
T. Appelquist, R.Pisarski, Phys.Rev. D**23** (1981) 2305
P. Ginsparg, Nucl.Phys. B**170** (1980) 388
- [11] M. Laine, Nucl.Phys. B**481** (1996) 43 (hep-ph/9605283)
- [12] G.R. Farrar, M. Losada, Phys.Lett. B**406** (1997) 60 (hep-ph/9612346)
M. Losada, Phys.Rev. D**56** (1997) 2893 (hep-ph/9605266)
- [13] J. Cline, K. Kainulainen, Nucl.Phys.B**482** (1996) 73 (hep-ph/9605235)
- [14] E. Akhmetzyanova, M. Dolgoplov, M. Dubinin, Phys.Rev. D**71** (2005) 075008 (hep-ph/0405264)
- [15] E. Akhmetzyanova, M. Dolgoplov, M. Dubinin, Phys.Part.Nucl. **37** (2006) 677
- [16] J.F. Gunion, H.E.Haber, Phys.Rev. D**67** (2003) 075019 (hep-ph/0207010)
M. Dubinin, A. Semenov, Eur.Phys.J. C**28** (2003) 223 (hep-ph/0206205)
F. Boudjema, A. Semenov, Phys.Rev. D**66** (2002) 095007 (hep-ph/0201219)
- [17] L. Vergara, Journal of Physics A**30** (1997) 6977
- [18] P.Amore, Journal of Physics A**38** (2005) 6463 (hep-th/0503142)
- [19] P. Amore, Journal of Mathematical Analysis and Applications **323** (2006) 63
M. Abramowitz and I. Stegun, Handbook of Mathematical Functions, Dover Publications, NY, 1964
- [20] H. Haber, R. Hempfling, Phys.Rev. D**48** (1993) 4280 (hep-ph/9307201)
- [21] S.Y. Choi, M. Drees, J.S. Lee, Phys.Lett. B**481** (2000) 57 (hep-ph/0002287)
- [22] J.C. Collins, *Renormalization*, Cambridge Univ. Press, Cambridge, 1984
- [23] E. Akhmetzyanova, M.Dolgoplov, M. Dubinin, Phys.Atom.Nucl. **70** (2007) 1549 (Yad.Fiz. **70** (2007) 1594)
- [24] C. Balazs, M. Carena, A. Menon, D.Morrissey, C.E.M. Wagner, Phys.Rev. D**71** (2005) 075002 (hep-ph/0412264)
S.Heinemeyer, M.Velasco, in: Proc.of 2005 ILC Workshop, Stanford, USA, hep-ph/0506267
- [25] M. Carena, J. Ellis, A. Pilaftsis, C. Wagner, Phys.Lett. B**495** (2000) 155 (hep-ph/0009212)
- [26] R. Gilmore, *Catastrophe theory for scientists and engineers*, John Wiley & Sons, New York-Chichester-Brisbane-Toronto, 1981
V.I. Arnold, *Critical points of smooth functions and their canonical forms*, Uspekhi Math. Nauk (USSR), **30** (1975) 3
R. Thom, *Structural stability and morphogenesis*, Reading, Benjamin, 1975
M. Morse, *The critical points of a function of n variables*, Trans. Am. Math. Soc., **33** (1931) 72

- [27] R. Peccei, H. Quinn, Phys.Rev.Lett. **38** (1977) 1440
- [28] A. Kusenko, P. Langacker, G. Segre, Phys.Rev. D**54** (1996) 5824 (hep-ph/9602414)
- [29] I. Affleck, M. Dine, Nucl.Phys. B**249** (1985) 361
- [30] S. Wolfram, *Mathematica* symbolic manipulation package, see <http://www.wolfram.com>
- [31] S. Chatrchyan et al. (CMS Collaboration), arXiv:1105.3152[hep-ex]; arXiv:1104.3168[hep-ex]; arXiv:1103.0953[hep-ex]; Phys.Lett. B698 (2011) 196 (arXiv:1101.1628[hep-ex]); Phys.Rev.Lett. 106 (2011) 011801 (arXiv:1011.5861[hep-ex])
- [32] S. Abdullin et al., Eur.Phys.J.C**39S2** (2005) 41

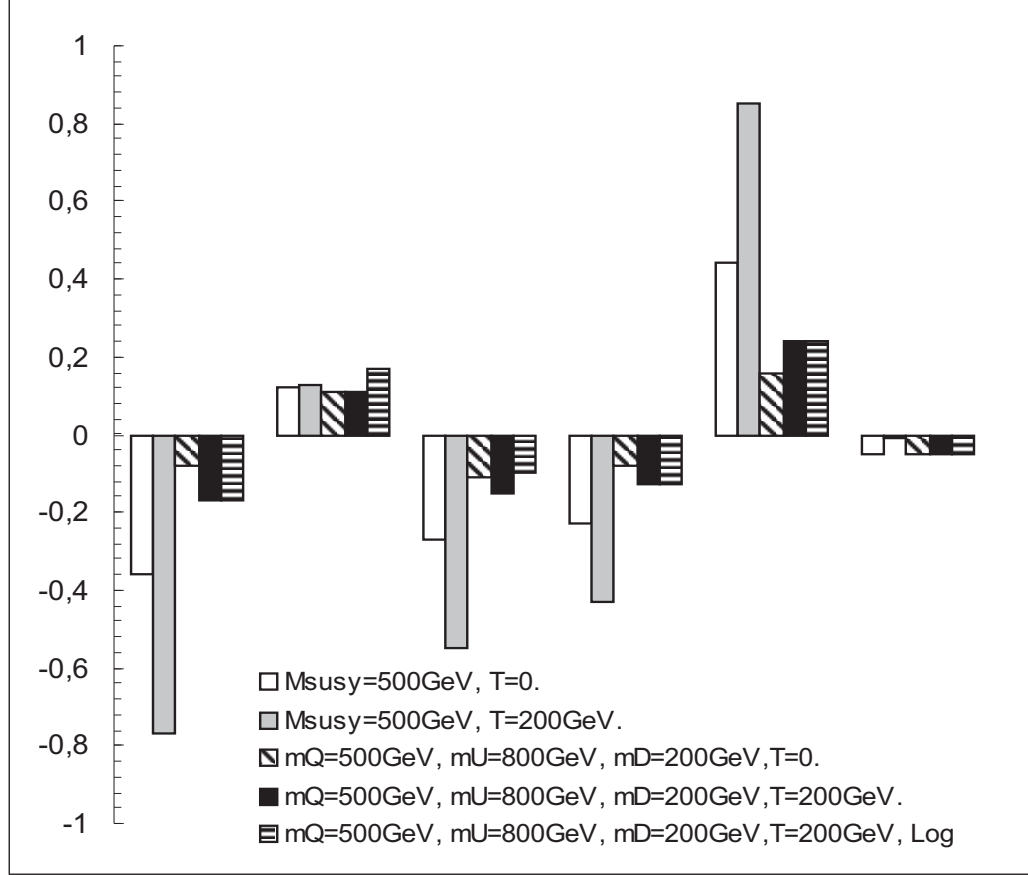


Figure 20: Histograms for temperature-dependent λ_i ($i=1, \dots, 7$) with various quantum corrections in the framework of the CPX-like scenario [25], $A_t = A_b = 1000$ GeV, $\mu = 2000$ GeV, in the cases of (a) degenerate squark masses $m_Q = m_t = m_b = M_{\text{SUSY}} = 500$ GeV, zero temperature, (b) degenerate squark masses $m_Q = m_t = m_b = M_{\text{SUSY}} = 500$ GeV, $T = 200$ GeV, (c) different squark masses $m_Q = 500$ GeV, $m_t = 800$ GeV, $m_b = 200$ GeV at zero temperature, and (d) different squark masses $m_Q = 500$ GeV, $m_t = 800$ GeV, $m_b = 200$ GeV at $T = 200$ GeV.

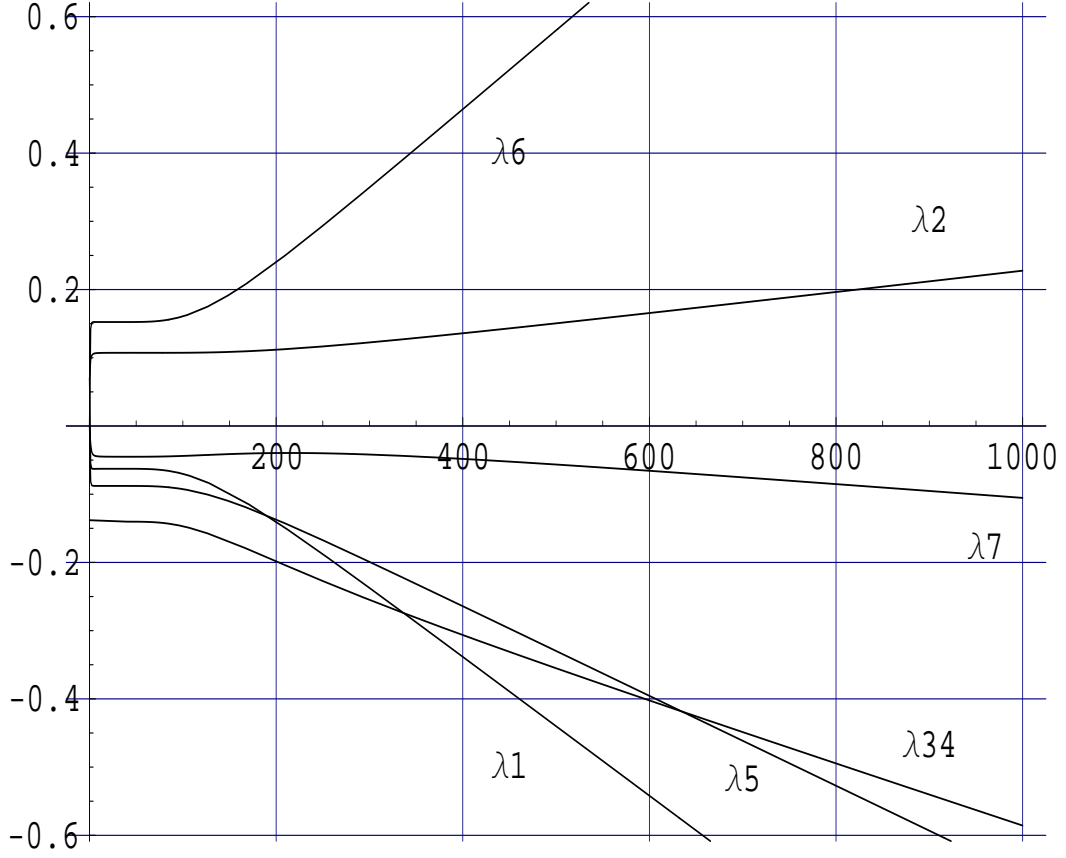
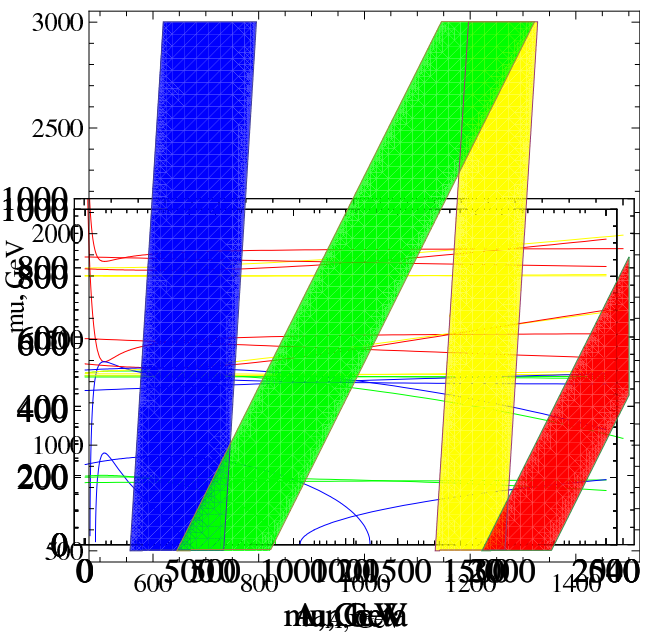
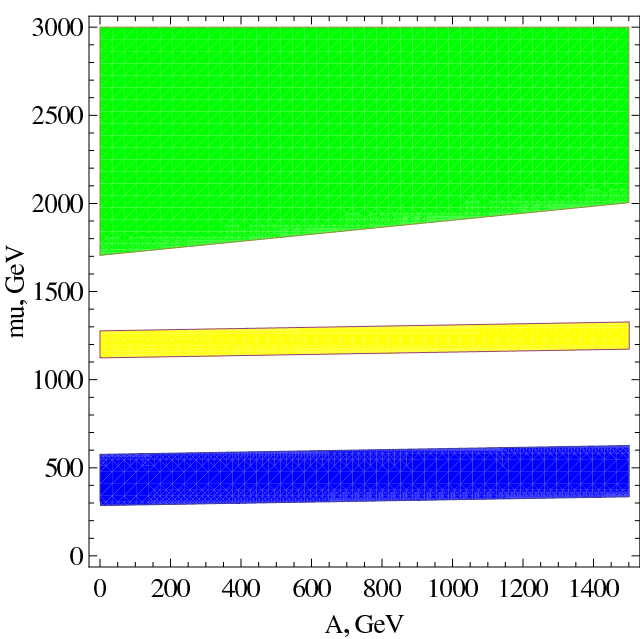
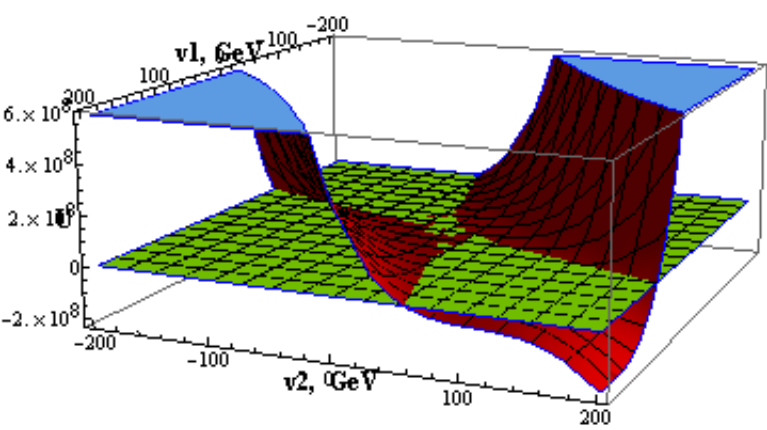
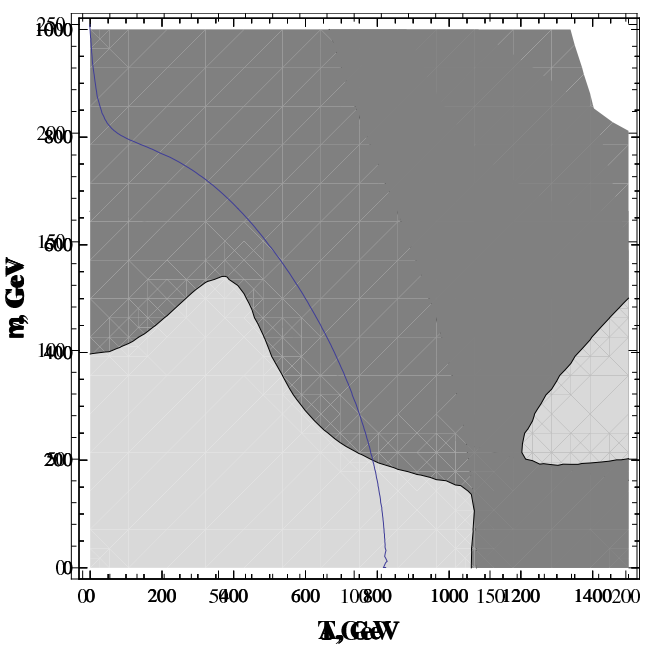


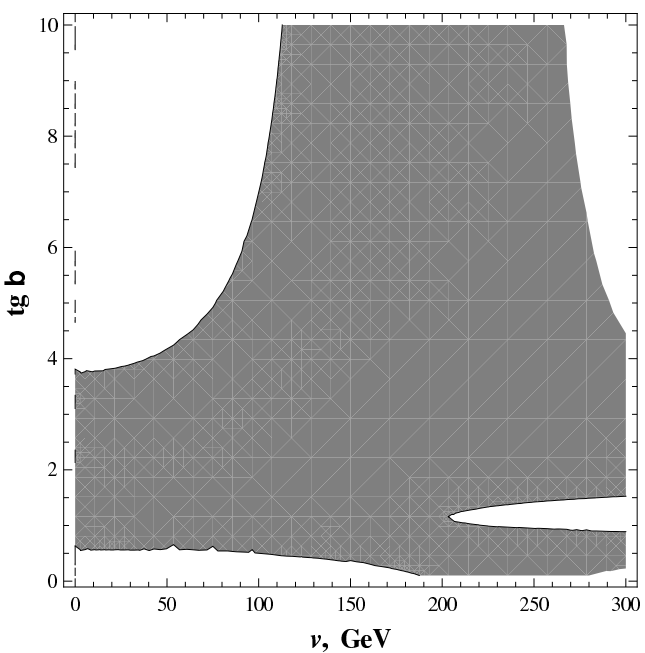
Figure 21: Effective temperature-dependent parameters λ_i ($i=1,\dots,7$) with the one-loop threshold and logarithmic corrections at $m_Z = 91.19$ GeV, $m_b = 3$ GeV, $m_t = 175$ GeV, $m_W = 79.96$ GeV, $g_2 = 0.6517$, $g_1 = 0.3573$, $G_F = 1.174 \cdot 10^{-5}$ GeV $^{-2}$, $M_{SUSY} = 500$ GeV, $m_Q = 500$ GeV, $m_t = 800$ GeV, $m_b = 200$ GeV, $\mu = 2000$ GeV, $A = X_t + \mu/\tan\beta$, $X_t = 700$ GeV, $\tan\beta = 5$, $h_t = 1$, $h_b = 0.1$.

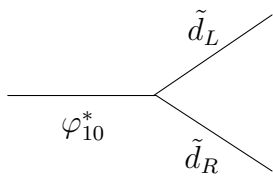




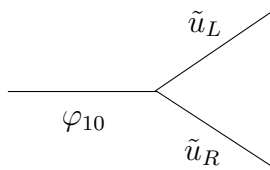




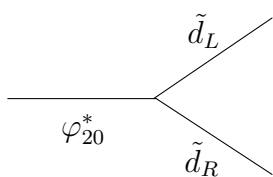




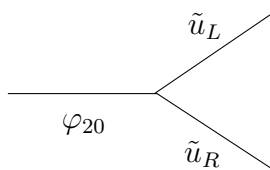
$h_D A_D$



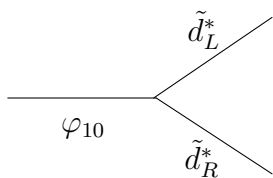
$-\mu^* h_U$



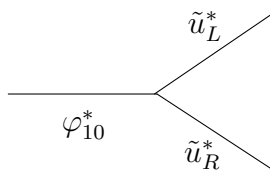
$-\mu^* h_D$



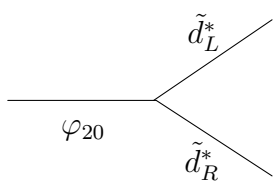
$h_U A_U$



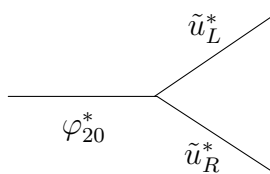
$h_D A_D^*$



$-\mu h_U$



$-\mu h_D$



$h_U A_U^*$